63-4-1

E74-63
APRIL 26, 1963

406 883

Thiokol
CHEMICAL CORPORATION
ELKTON DIVISION

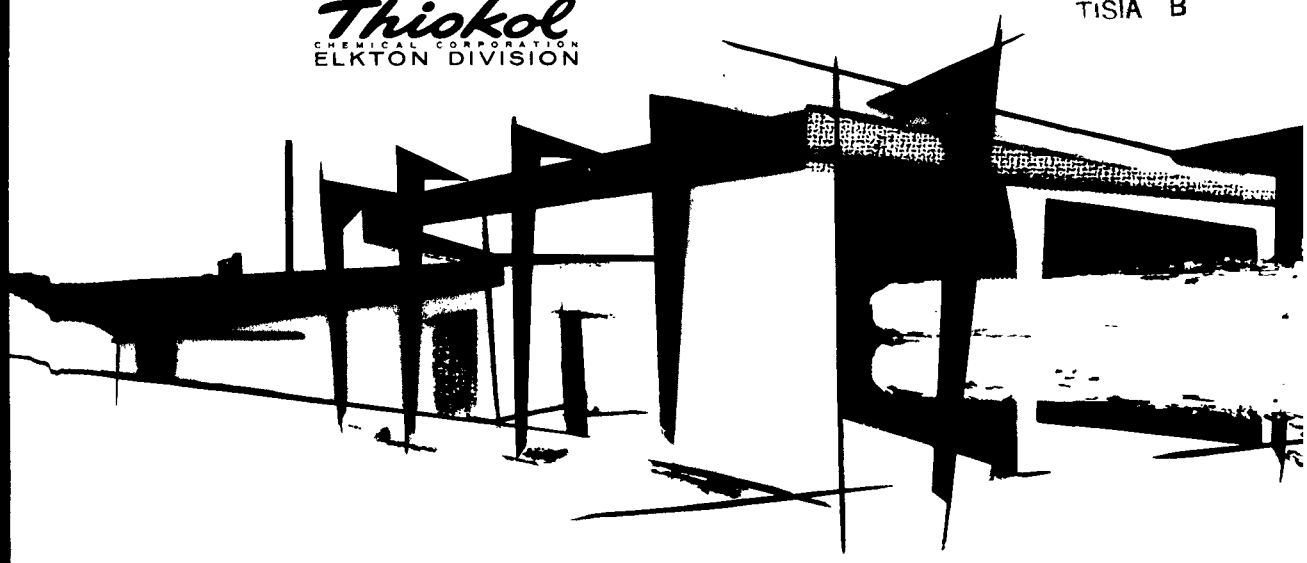

QUARTERLY PROGRESS REPORT NO. 3, A RESEARCH STUDY TO ADVANCE THE STATE OF THE ART OF SOLID PROPELLANT GRAIN DESIGN, CONTRACT AF 33(616)-6530, SUPPLEMENT NO. 6

E74-63

THIOKOL CHEMICAL CORPORATION
ELKTON DIVISION
ELKTON, MARYLAND

QUARTERLY PROGRESS REPORT NO. 3

JANUARY 1, 1963, TO APRIL 1, 1963

"A RESEARCH STUDY TO ADVANCE THE STATE OF THE ART OF SOLID PROPELLANT GRAIN DESIGN"

CONTRACT NO. AF 33(616)-6530

SUPPLEMENT AGREEMENT NO. 6

PROJECT NO. 3059

TASK NO. 30531

PREPARED FOR:

ROCKET PROPULSION LABORATORY (DGSMD)
AIR FORCE SYSTEMS COMMAND
UNITED STATES AIR FORCE
EDWARDS, CALIFORNIA

APRIL 26, 1963

H. G. Jones
General Manager

FOREWORD

This report has been prepared by the Elkton Division of Thiokol Chemical Corporation for the Rocket Propulsion Laboratory (DGSMD) at Edwards, California. Lt. Harold W. Gale is the Air Force Project Officer. The report is based on the work accomplished during the period from January 1, 1963, to April 1, 1963, under Supplemental Agreement No. 6 to Contract AF 33(616)-6530, an engineering research program to develop advanced methods for improving the state of the art of solid propellant grain design.

The principal contributors to this report are Messrs. W. G. Andrews, D. H. Frederick, F. E. Moore, D. Saylak, A. Stornelli, D. D. Thomas and R. H. Thompson. Mr. James F. Hoebel is the Program Manager.

TABLE OF CONTENTS

LIST OF TABLES

LIST OF FIGURES

LIST OF FIGURES (Continued)

ABSTRACT

The work conducted under Contract AF 33(616)-6530 during the period from January 1, 1963, to April 1, 1963, is reported. This program is a research study to advance the state of the art of solid propellant grain design and consists primarily of theoretical and applied analyses of solid propellant grain designs, considering in particular heat transfer effects, propellant slump, and the effect of strain on burning rate.

An analytical study is being undertaken to develop a two-dimensional heat transfer analysis for solid propellant motors subjected to a nonlinear external thermal environment. The application of this analysis to the Advanced Grain Design Computer Program, previously developed under this contract, is also being investigated to determine thermal effects upon ballistic characteristics.

The programming of the two-dimensional heat transfer analysis was completed, and several test cases were evaluated. A severe stability requirement is imposed on the solution resulting from the consideration of a thin case wall having a relatively higher thermal diffusivity.

The input and output sections of the Advanced Grain Design Computer Program were modified, and certain changes involved with the application of a variable grain temperature profile to the program were installed.

The effect of strain on the burning rates of several propellants was investigated. This effect increases as the deviation from incompressible behavior increases.

The analysis of propellant slump involved a preliminary analysis of a finite length, cylindrical grain having a spherical head end and under acceleration in the longitudinal direction. Boundary conditions were considered and the relevant finite difference equations were developed.

SUMMARY

Contract AF 33(616)-6530 is directed toward the development of new and unique methods for the design and evaluation of solid propellant grains. The studies undertaken include theoretical and applied analyses of solid propellant grain design from the standpoint of ballistic and physical properties of propellants.

The current program is divided into three areas of study: (1) a heat transfer analytical study, (2) the effect of strain on burning rate, and (3) propellant slump analysis.

The major accomplishments during the period from January 1, 1963, to April 1, 1963, in each of these areas are summarized in the following three sections.

I. HEAT TRANSFER ANALYSIS

The two-dimensional heat transfer analysis was completely programmed. Preliminary evaluation of the program indicated that thin case walls impose severe stability requirements upon the analysis and result in extremely long computation times. The results for two center-perforated grains are presented. Some modifications to the program have been made to correct an error in the finite difference equations to the temperature at an internal surface point on an irregular boundary.

The Advanced Grain Design Computer Program input data generator was modified to increase accuracy, simplify the required input data, and make the program more fully "fail proof." The output was revised and now provides check results.

The analysis of solid propellant rocket motors having a variable grain temperature profile has been applied to the Advanced Grain Design Computer Program. Although only one half star point of the grain may be presently analyzed, this is sufficient for debugging purposes.

II. EFFECT OF STRAIN ON BURNING RATE

Four propellants were investigated by determining the effect of strain on Poisson's ratio and then relating that parameter to any changes in burning rate. There appears to be a correlation between the deviation from incompressible behavior and the effect of strain on burning rate. This could permit a prediction of the effect of strain on burning rate by an examination of Poisson's ratio at that strain.

III. PROPELLANT SLUMP ANALYSIS

The specification of the finite difference equations and boundary conditions associated with the elastic stress function analysis of an axisymmetrical cylindrical propellant charge that is capped by a spherical head end was accomplished. It is assumed that the grain is under a constant body force in the longitudinal direction and that the grain is bonded to a rigid case.

I. INTRODUCTION

This is the third quarterly report submitted in partial fulfillment of continuation studies under Contract AF 33(616)-6530, Supplement No. 6, Project 3059, Task 30531, "A Research Study to Advance the State of the Art of Solid Propellant Grain Design," and summarizes the results of work performed during the period from January 1, 1963, to April 1, 1963. Effort on this contract supplement was initiated on July 1, 1962, and is scheduled to terminate on May 31, 1963.

The objective of this program is to advance the state of the art of solid propellant grain design from a mechanical as well as ballistic standpoint.

Previous studies under this contract have included the development of a generalized computer program to evaluate the ballistics of any internal burning, singly connected propellant grain including consideration of head- and aft-end effects on the burning surface area. The effect of propellant defects on ballistic performance was studied using windowed test motors and bombs containing propellant with artificially prepared voids and cracks. A strain analysis was performed of solid propellant motors under steady-state thermal loading employing the PhotoStress technique. Experimental studies were also made to investigate the feasibility of using an analogous electrical network in the solution of solid propellant heat conduction problems.

The current program has been divided into three areas of investigations:

(1) Heat Transfer Analysis

(2) Effect of Strain on Burning Rate

(3) Propellant Slump Analysis

II. HEAT TRANSFER ANALYSIS

A. Two-Dimensional Heat Transfer Analysis

An analytical study is being performed under this phase to consider applications and the correlation of the heat transfer analysis with the Advanced Grain Design Computer Program to determine the characteristics of solid propellant motors under nonlinear external heating conditions.

Principal effort this quarter has been directed toward completion of the program and the evaluation of numerous test cases.

The program has been written and consists of two sections. Section I reads the input data from tape and writes the initial output on tape. Section II computes the temperature profile at each time increment and writes the profile on tape as output for each of the specified print intervals.

Several test cases were evaluated, two of which produced results immediately usable by the Rocket Propulsion Laboratory. Test cases containing an irregular internal boundary failed and brought to light minor errors in the basic analysis and program logic; these have been corrected.

A significant result obtained from the initial test case was the severe stability requirements imposed on the solution by a thin case wall having a relatively higher thermal diffusivity than the propellant. These stability requirements result in small iteration times and consequently long computation times. Since the validity of the case wall and case-propellant temperature relationships was demonstrated within the program, the remaining test cases were evaluated without a case material.

1. Test Case Evaluation

In the evaluation of the program, several test cases were considered. There was sufficient variation among the test cases so that each particular routine within the program was evaluated. Each test case is described below and illustrated in Figures 1 through 5, respectively.

(1) A center perforated grain with a thin steel case wall. The center perforation was extremely small in order to approximate an end burning grain. The external boundary conditions were as follows:

$$q = E \cos \phi = 400 \cos \phi \quad \frac{Btu}{hr\ ft^2}; \quad \phi = 0° - 90°$$

$$q = \mathcal{F}_o\, \sigma\, (T_{rad}^4 - T_{os}^4) = 0.3\sigma(100^4 - T_{os}^4)\ \frac{Btu}{hr\ ft^2}; \quad \phi = 90° - 180°$$

The internal boundary condition was adiabatic.

(2) (a) Same as (1) without the case wall.

(b) Same as (2) (a) with the following external boundary conditions:

$$q = E \cos \phi = 120 \cos \phi \quad \frac{Btu}{hr\ ft^2}; \quad \phi = 0° - 90°$$

$$q = \mathcal{F}_o\, \sigma\, (T_{rad}^4 - T_{os}^4) = 0.3\sigma\, (100^4 - T_{os}^4)\ \frac{Btu}{hr\ ft^2}; \quad \phi = 90° - 180°$$

(3) A 30° segment of a star grain with no case wall. The external boundary condition was:

$$q = h_o\, (T_{conv} - T_{os}) = 8.5\ (580 - T_{os})\ \frac{Btu}{hr\ ft^2}; \quad \phi = 0° - 30°$$

The internal boundary condition was:

$$q = h_i\, (T_{conv} - T_{os}) = 0.25\ (580 - T_{os})\ \frac{Btu}{hr\ ft^2}$$

(4) A 180° segment of the same star grain considered in (3).

The external boundary condition was:

A4868

Case Properties

Thermal Conductivity = 22 Btu/Hr-Ft-°R
Specific Heat = 0.11 Btu/Lb-°R
Density = 490 Lb/Ft^3
Initial Temperature = 530 °R

Propellant Properties

Thermal Conductivity = 0.14 Btu/Hr-Ft-°R
Specific Heat = 0.39 Btu/Lb-°R
Density = 100.22 Lb/Ft^3
Initial Temperature = 530°R

σ = Stefan-Boltzmann Constant
= 0.173×10^{-8} Btu/Hr-Ft^2-°R^4

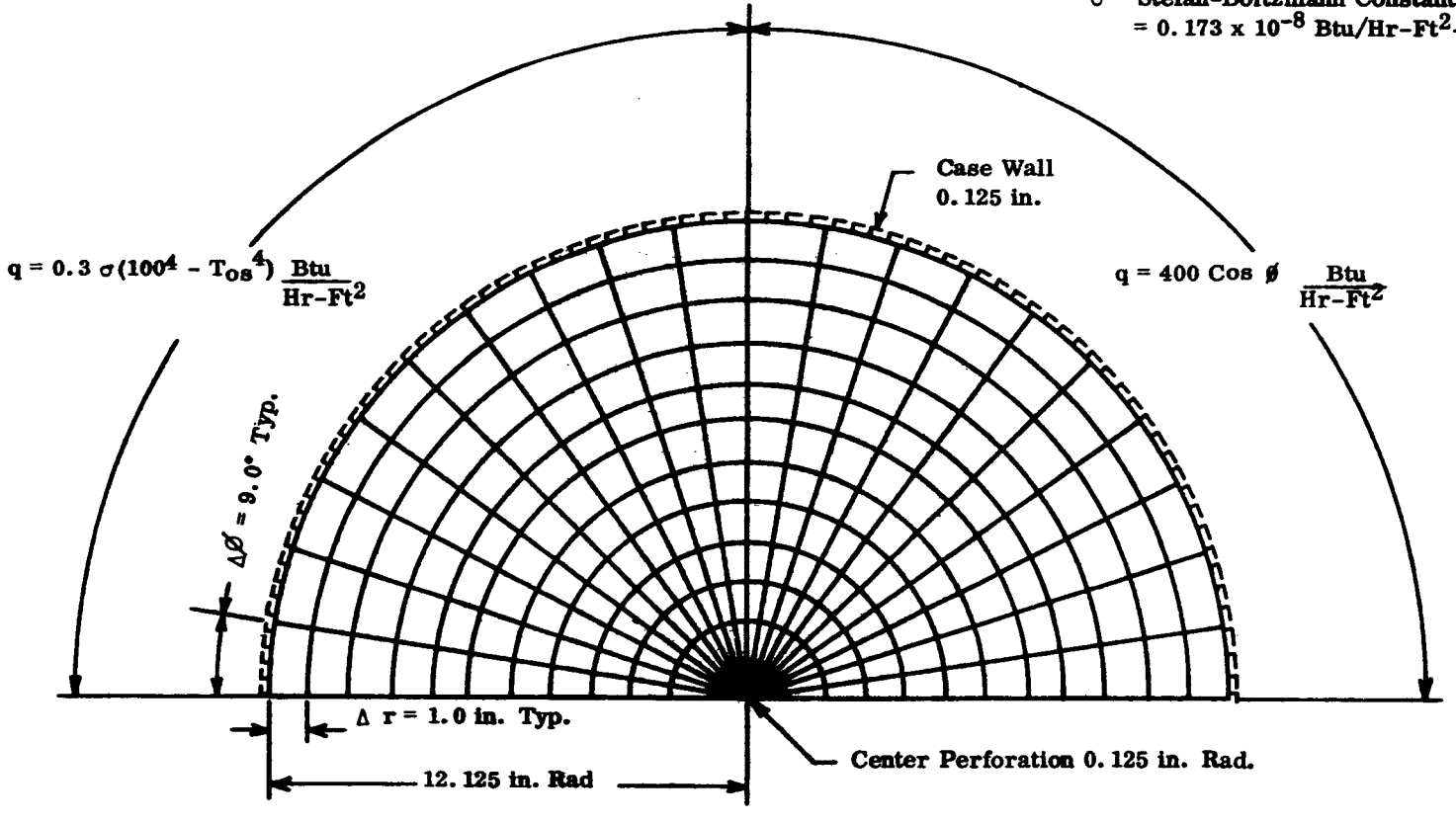

FIGURE 1. NODAL NETWORK AND BOUNDARY CONDITIONS FOR TEST CASE (1)

A4870

No Case Wall

Propellant Properties

Thermal Conductivity = 0.14 Btu/Hr-Ft-°R
Specific Heat = 0.39 Btu/Lb-°R
Density = 100.22 Lb/Ft^3
Initial Temperature = 530°R

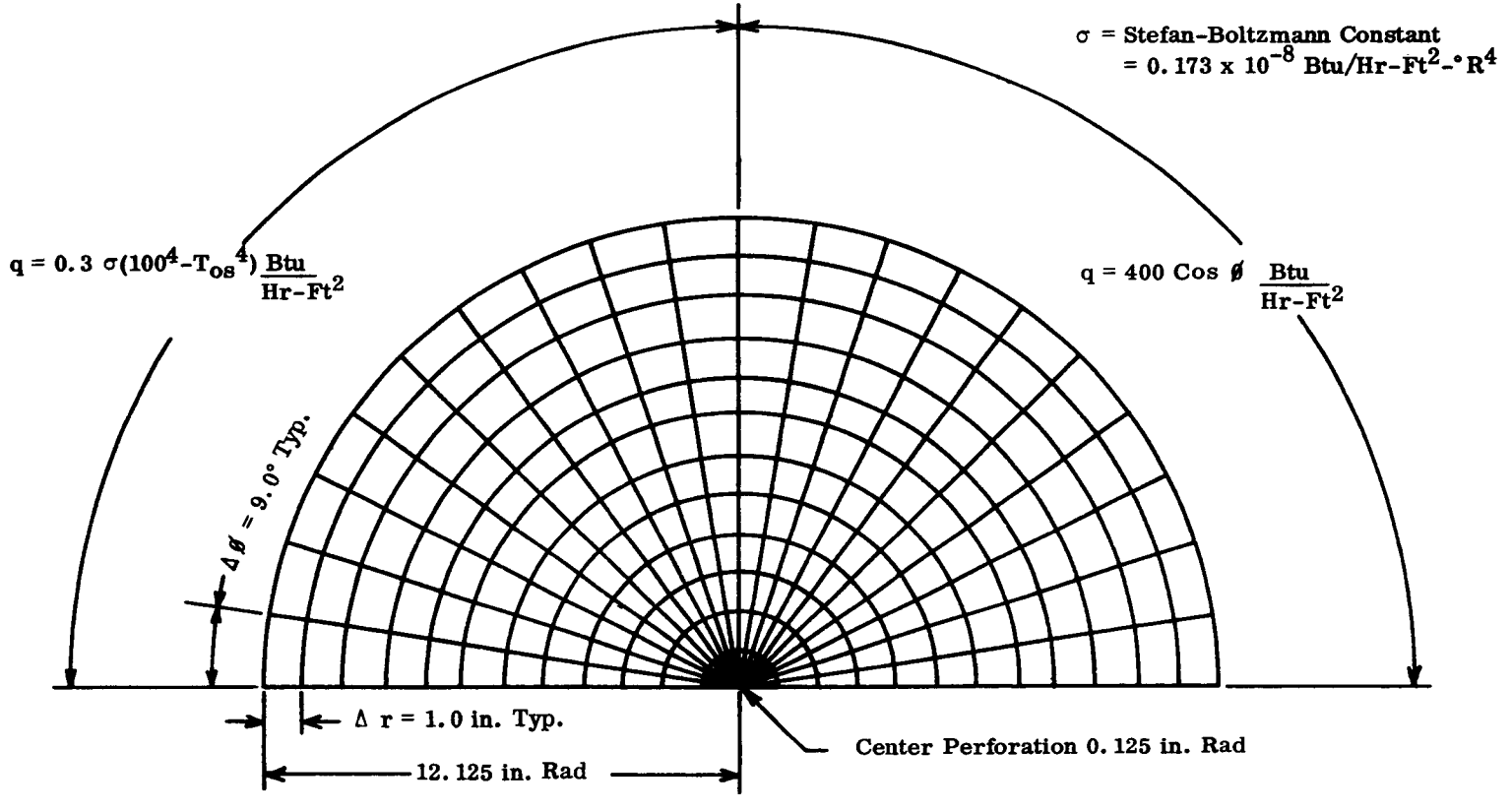

FIGURE 2. NODAL NETWORK AND BOUNDARY CONDITIONS FOR TEST CASE (2) (a)

A4871

No Case Wall

Propellant Properties

Thermal Conductivity	= 0.14 Btu/Hr-Ft-°R
Specific Heat	= 0.39 Btu/Lb-°R
Density	= 100.22 Lb/Ft^3
Initial Temperature	= 530°R

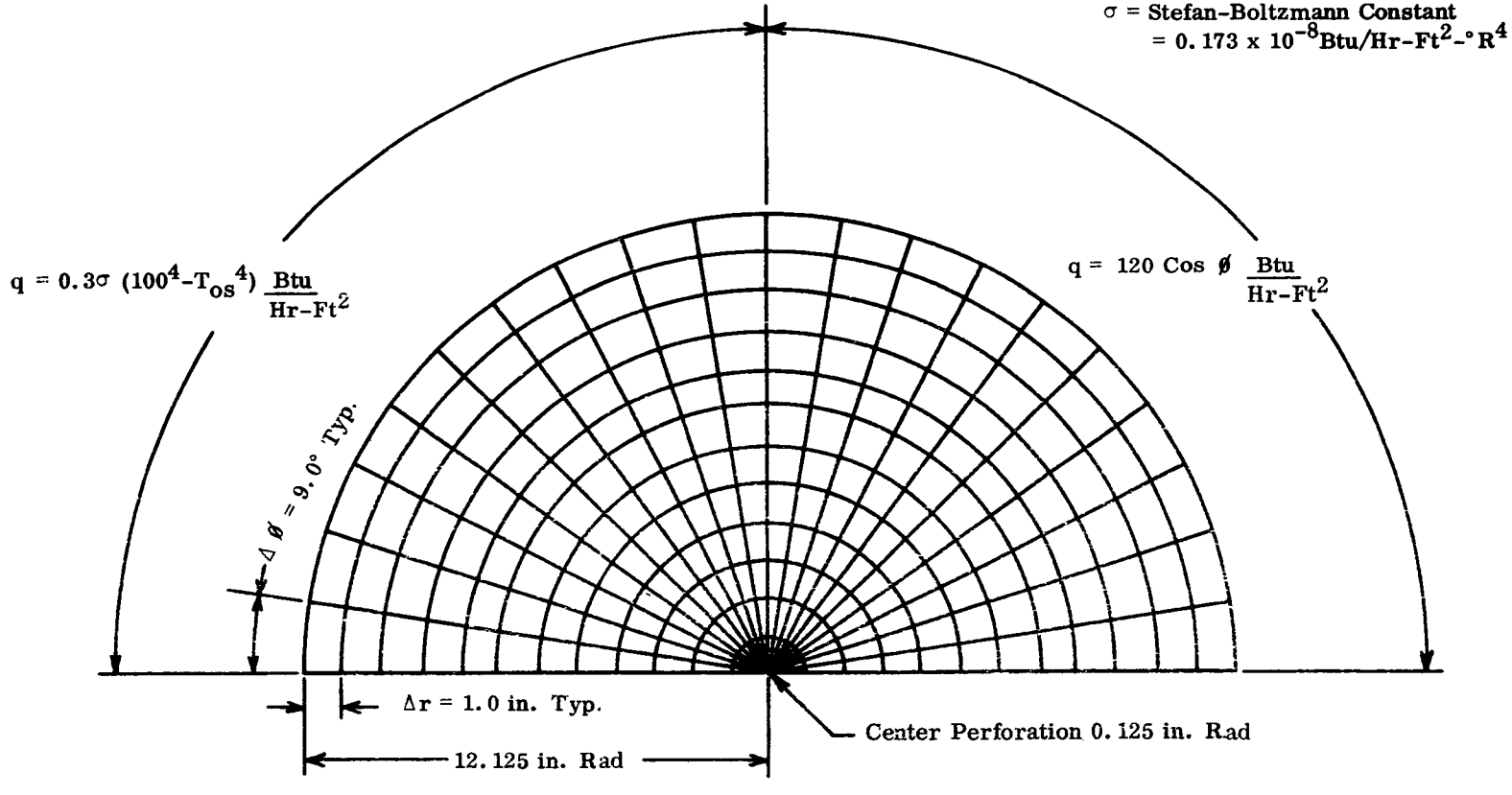

FIGURE 3. NODAL NETWORK AND BOUNDARY CONDITIONS FOR TEST CASE (2) (b)

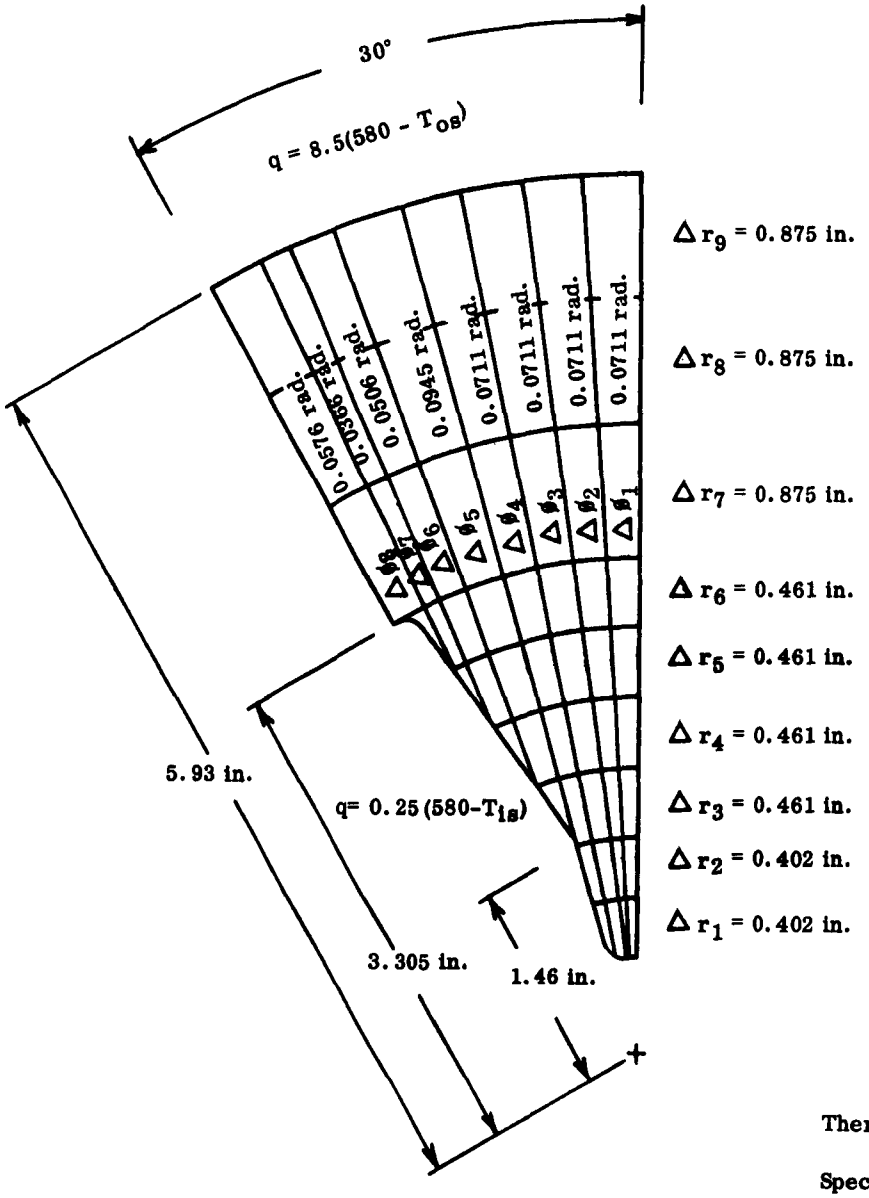

Propellant Properties

Thermal Conductivity = 0.249 $\frac{\text{Btu}}{\text{Hr-Ft}}$

Specific Heat = 0.237 $\frac{\text{Btu}}{\text{Lb-°R}}$

Density = 108.84 $\frac{\text{Lb}}{\text{Ft}^3}$

Initial Temperature = 460° R

FIGURE 4. NODAL NETWORK AND BOUNDARY CONDITIONS FOR TEST CASE (3)

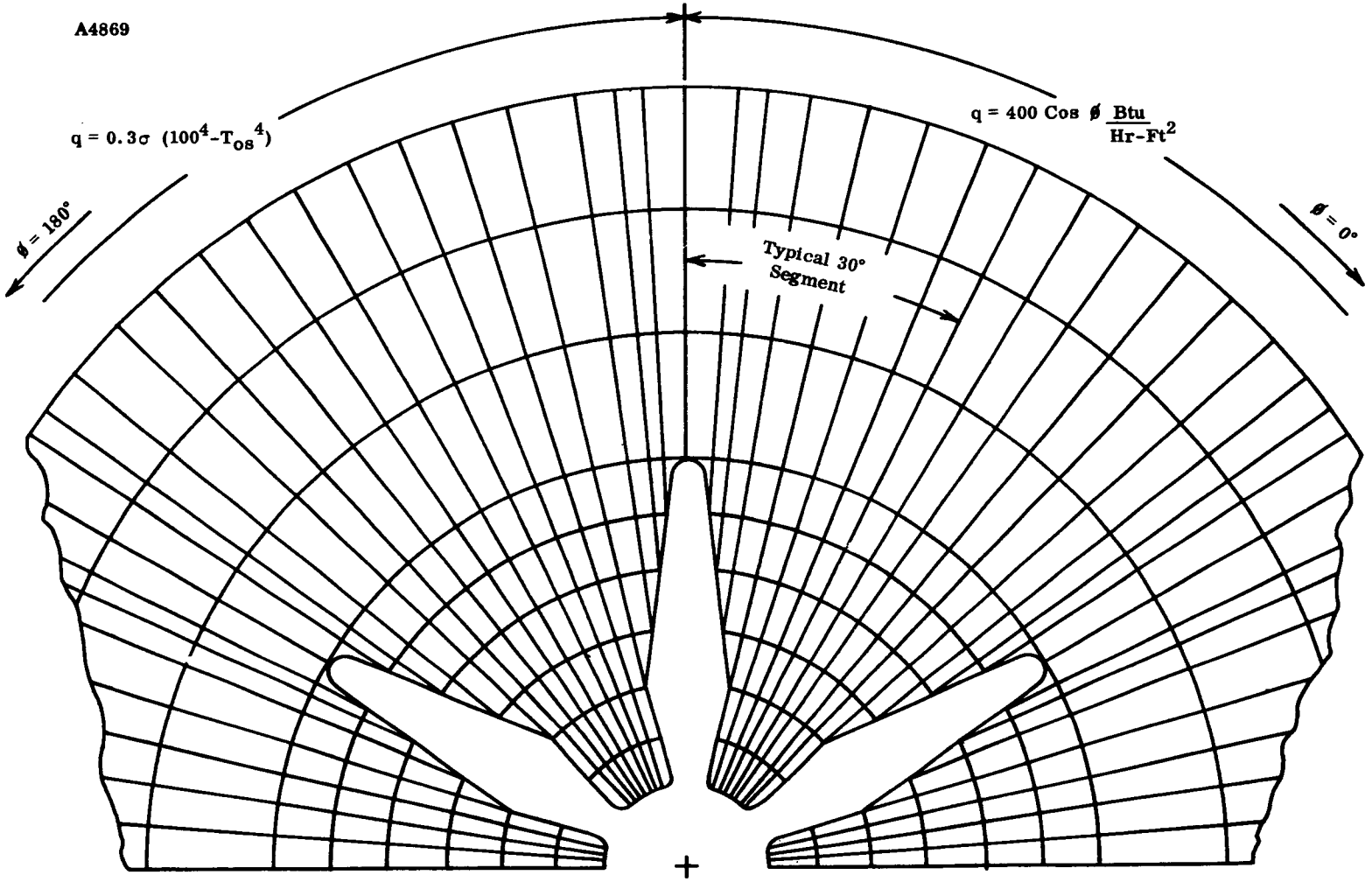

FIGURE 5. NODAL NETWORK AND BOUNDARY CONDITIONS FOR TEST CASE (4)

$$q = E \cos \phi = 400 \cos \phi \ \frac{Btu}{hr\ ft^2};\ \phi = 0 - 90°$$

$$q = \mathcal{F}_o \sigma (T_{rad}^4 - T_{os}^4) = 0.3 \sigma (100^4 - T_{os}^4) \ \frac{Btu}{hr\ ft^2};\ \phi = 90° - 180°$$

The internal boundary condition was adiabatic.

2. Discussion

Test case 1 served to evaluate the external surface and case-propellant interface nodal point relationships; but due to the excessive running time caused by the severe stability requirements, no further information was obtained. Specifically, the high thermal diffusivity and small thickness of the case wall in relation to the propellant required an extremely small time increment to maintain a stable solution.

Minimum stability is maintained by using a time increment that permits the coefficient of the local nodal point temperature ($T_{j,k}$) to be greater than zero. Thus, the stability equations for the outer surface and propellant internal nodes, respectively, are given as follows:

Outer Surface Nodes:

$$1 - \frac{\Delta \theta}{\rho C_p} \left[\left(\frac{K_{j,k} - K_{j-1,k}}{2 \Delta r_2} \right) \left(\frac{h_o}{K_{j,k}} + \frac{\mathcal{F}_o \sigma}{K_{j,k}} T_{os}^3 - \frac{1}{\Delta r_2} \right) \right.$$

$$+ \left(\frac{K_{j,k+1} - K_{j,k-1}}{r_{j,k}^2 (\Delta \phi_1 + \Delta \phi_2)} \right) \left(\frac{1}{\Delta \phi_1} - \frac{1}{\Delta \phi_2} \right) + \left(\frac{K_{j,k} + K_{j-1,k}}{2 \Delta r_2} \right) \left(\frac{h_o}{K_{j,k}} + \frac{\mathcal{F}_o \sigma}{K_{j,k}} T_{os}^3 + \frac{1}{\Delta r_2} \right)$$

$$\left. + \left(\frac{K_{j,k} + K_{j-1,k}}{4 r_{j,k}} \right) \left(\frac{h_o}{K_{j,k}} + \frac{\mathcal{F}_o \sigma}{K_{j,k}} T_{os}^3 - \frac{1}{\Delta r_2} \right) \right] \geq 0$$

Internal Nodes:

$$1 - \frac{\Delta\theta}{\rho C_p}\left[\left(\frac{K_{j+1,k} - K_{j,k}}{\Delta r_1 + \Delta r_2}\right)\left(\frac{1}{\Delta r_1} - \frac{1}{\Delta r_2}\right) + \left(\frac{K_{j,k+1} - K_{j,k-1}}{r_{j,k}^2 (\Delta\phi_1 + \Delta\phi_2)}\right)\left(\frac{1}{\Delta\phi_1} - \frac{1}{\Delta\phi_2}\right)\right.$$

$$+ \left(\frac{K_{j+1,k} + K_{j-1,k}}{\Delta r_1 + \Delta r_2}\right)\left(\frac{1}{\Delta r_1} + \frac{1}{\Delta r_2}\right) + \left(\frac{K_{j+1,k} + K_{j-1,k}}{4 r_{j,k}}\right)\left(\frac{1}{\Delta r_1} + \frac{1}{\Delta r_2}\right)$$

$$\left. + \left(\frac{K_{j,k+1} + K_{j,k-1}}{r_{j,k}^2 (\Delta\phi_1 + \Delta\phi_2)}\right)\left(\frac{1}{\Delta\phi_1} + \frac{1}{\Delta\phi_2}\right)\right] \geq 0$$

Stability restrictions for the propellant case interface nodes fall between the above two relationships and should present no problem when the maximum of these is used.

For test case 1, the ratio of the time increment required by the propellant interior points to that required by the external surface points was approximately 10^3.

In an attempt to reduce the computation time and retain the case material, the following procedure was outlined and included within the program.

A basic or minimum time increment is selected, based upon the outer surface stability requirement. Iterations are performed about the case for the outer surface and case-propellant interface points alone. This is continued until the number of iterations about the case times the basic time interval is less than, or equal to, the time interval satisfying the internal point stability requirements. Therefore, if the basic time interval is $\Delta\theta_B$, the time interval for the internal point iterations is

$N\Delta\theta_B$, where N is the number of iterations through the outer surface and interface point.

In this manner, the total number of points considered is reduced since only the case is being considered, stability is satisfied at all points, and no loss in accuracy of results is imposed. Although some decrease in computational time was realized, a significant reduction was not realized by this technique. Consequently, further test cases were evaluated without a case wall, which constitutes an assumption of a thermally thin case and/or a case with material properties closely resembling that of the propellant. Inasmuch as the case wall-propellant interface calculations had been effectively checked out, this is sufficient for test purposes.

Test cases (2) (a) and (2) (b) were successfully evaluated, and the resulting temperature distributions after 12 hours at the specified environment are shown in Figures 6 and 7. Intermediate profiles corresponding to every 0.5 hours were also obtained.

Upon attempting to evaluate test case 3, difficulty was encountered in computing the internal boundary temperatures. The routines within the program and the corresponding finite difference equations used to compute these points were reviewed. A discrepancy was noted in the manner in which the basic heat conduction equation was modified to account for an iteration entering propellant on constant r and entering propellant on constant ϕ across an irregular internal boundary.

These modifications were corrected to the following:

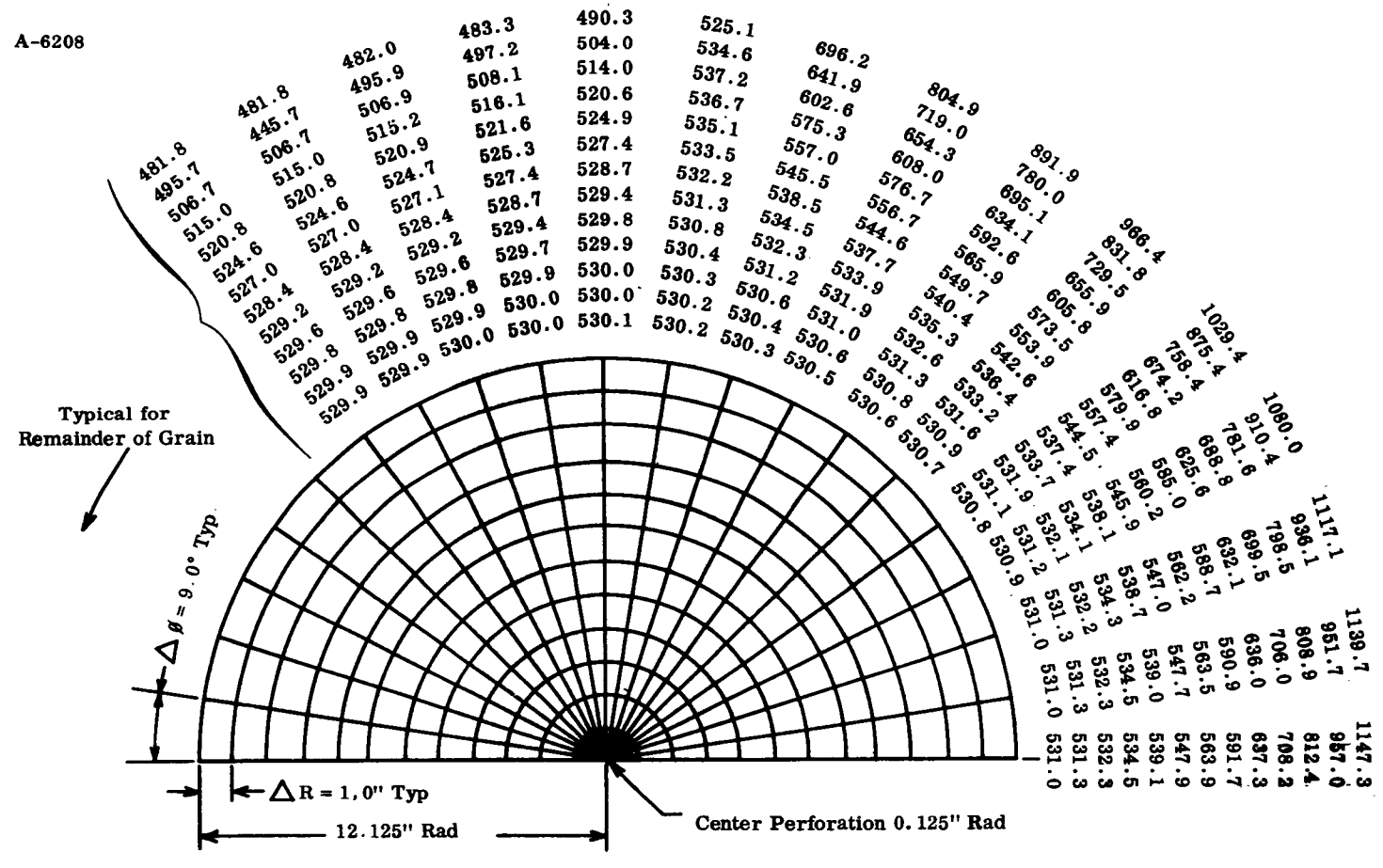

FIGURE 6. TEMPERATURE DISTRIBUTION THROUGH GRAIN AFTER 12 HOURS FOR TEST CASE 2(a)

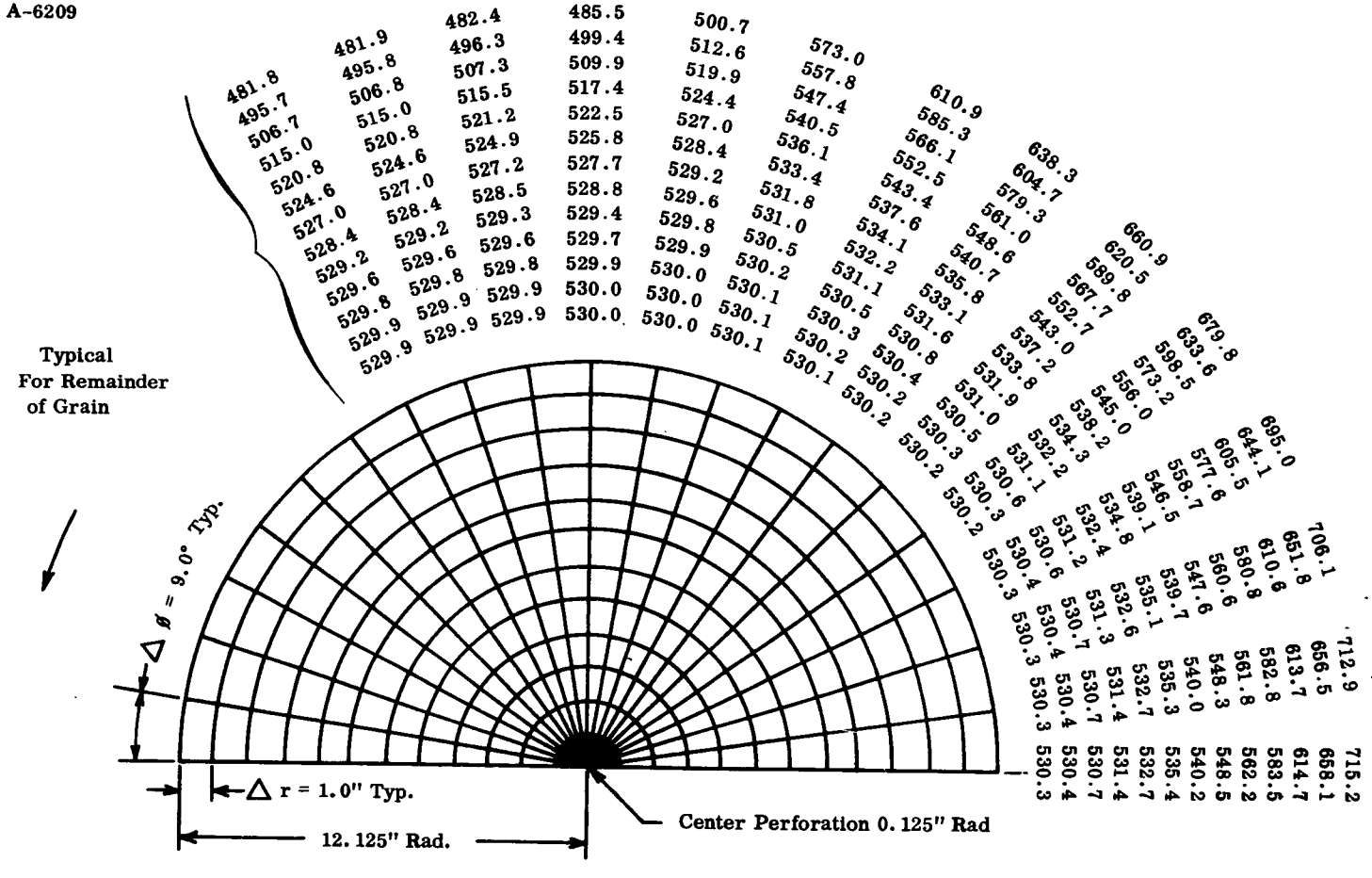

FIGURE 7. TEMPERATURE DISTRIBUTION THROUGH GRAIN AFTER 12 HOURS FOR TEST CASE 2 (b)

(1) Entering propellant on constant $\phi \Rightarrow$*. Replace backward differences in r as follows:

$$\frac{T_{j,k} - T_{j-1,k}}{\Delta r_2} = \frac{h_i}{K_{j,k}} (T_{j,k} - T_c) \left[1 + \frac{1}{r_j^2} \left(\frac{\Delta r}{\Delta \phi} \right)^2 \right]^{-1/2}$$

and $\Delta r_2 = \Delta r_1 \qquad K_{j-1,k} = K_{j+1,k}$

(2) Entering propellant on constant $r \Rightarrow$, Replace backward differences in ϕ as follows:

$$\frac{T_{j,k} - T_{j,k-1}}{\Delta \phi_2} = \frac{h_i}{K_{j,k}} (T_{j,k} - T_c) \left[1 + r_j^2 \left(\frac{\Delta \phi}{\Delta r} \right)^2 \right]^{-1/2}$$

and $\Delta \phi_2 = \Delta \phi \qquad K_{j,k-1} = K_{j,k+1}$

These corrections within the program have been undertaken, and a satisfactory evaluation of the remaining test cases should be available during the early part of the next reporting period.

For the test cases considered, the heat transfer program performance has been satisfactory. The long computational time experienced on the test case having a thin case wall is characteristic of a single-channel 7070. On either a multichannel system or an internally faster processing computer, this running time would not be excessively long. In reality, the evaluation of the temperature-time

*$\Rightarrow$ Means "Implies"

history for the various imposed environments would not be an imposing problem with the current 7070 computer. However, for program development purposes, inclusion of the case wall does result in inefficient use of computer time.

It can be concluded that the program is progressing on schedule, and evaluation of the remaining test cases should be completed during the first part of the next quarter. At that time final documentation of the program will be undertaken.

B. Modification of the Advanced Grain Design Computer Program

The perfection of the uniform grain temperature Advanced Grain Design Analysis is a continuing effort. During this reporting period, the input and output sections of the program were reworked.

The input data generator was modified to increase accuracy, simplify the required input data, and make the program more fully "fail proof." Figure 8 illustrates the generalized rocket motor parameters required by the new input data generator. The nomenclature for this program is listed in Table I.

A complete rocket motor test case was evaluated. The motor is shown schematically in Figure 9, while Tables II through XI are reproductions of the output. These tables are described in the following paragraphs.

Table II - The first page of computer output simply lists the input data exactly as it appears on the input data cards, but with variable names printed above each word.

Tables III, IV, and V are what is called the "Tape 3" output. Tape 3 is the magnetic tape that contains the coordinates and angles between normals of the corner

TABLE I

NOMENCLATURE*

A - Relative to Computer Output

I-XX	Moment of inertia about X axis =	$\int Y^2 + Z^2 \, dm$
I-YY	Moment of inertia about Y axis =	$\int X^2 + Z^2 \, dm$
I-ZZ	Moment of inertia about Z axis =	$\int X^2 + Y^2 \, dm$
I-XY	"XY" product of inertia =	$- \int XY dm$
I-XZ	"XZ" product of inertia =	$- \int XZ dm$
I-YZ	"YZ" product of inertia =	$- \int YZ dm$

X, Y, Z — Coordinates of cartesian frame oriented (as shown in Figure 10) with Z corresponding to the motor axis

R, Θ, Z — Coordinates of polar frame oriented relative to XYZ above through: $R = \sqrt{X^2 + Y^2}$; $\theta = \text{Tan}^{-1} (Y/X)$ Z = Z

S-Y, S-H, H-S — Angles between normals to the initial burning surface as shown in Figures 10 and 11

*All linear dimensions are in inches.
All angular dimensions are in degrees.
All weights are in lbs.

NOMENCLATURE

B - Relative to Computer Input

(These symbols are also identified in Figure 8)

R_{ch}	Ellipse ratio of case head ellipse
Z_{ch}	Z translation of center of case head ellipse
A_{ch}	Major axis of case head ellipse
R_{ca}	Ellipse ratio of case aft ellipse
Z_{ca}	Z translation of center of case aft ellipse
A_{ca}	Major axis of case aft ellipse
D_{port}	Diameter of igniter port
Z_{aft}	Distance from Z = 0 to aft cutback
R_1, R_2, R_3	Fillet radii in grain cross section
T_1	Least port diameter
T_3	Greatest port diameter
N	Number of star points

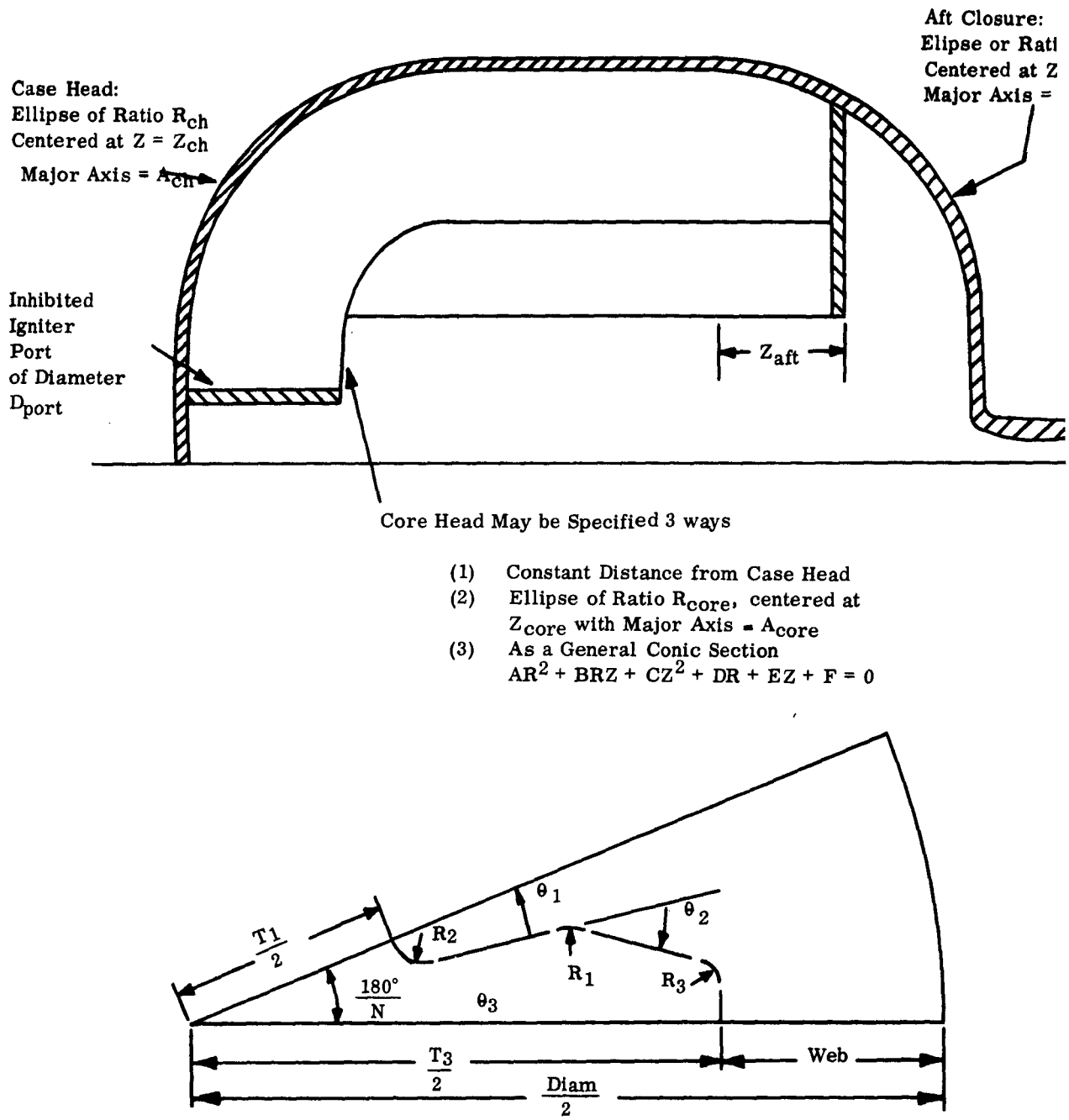

FIGURE 8. SCHEMATIC REPRESENTATION OF CROSS SECTIONS OF GENERALIZED SOLID PROPELLANT ROCKET AMENABLE TO SOLUTION WITH AGDA SHOWING REQUIRED INPUT PARAMETERS

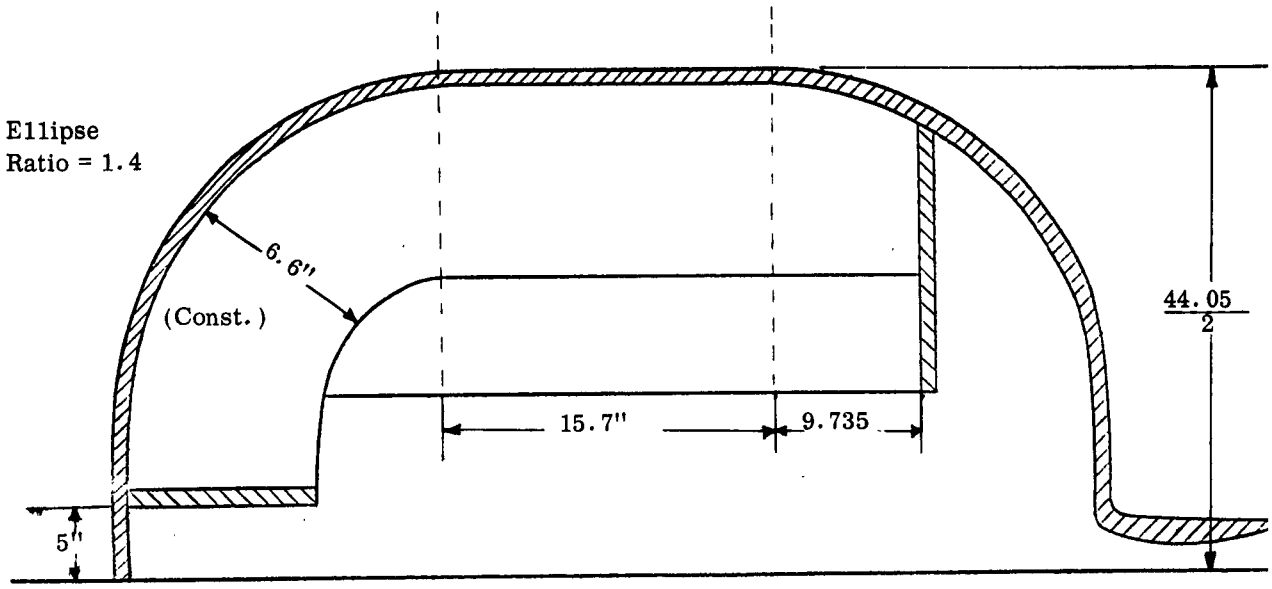

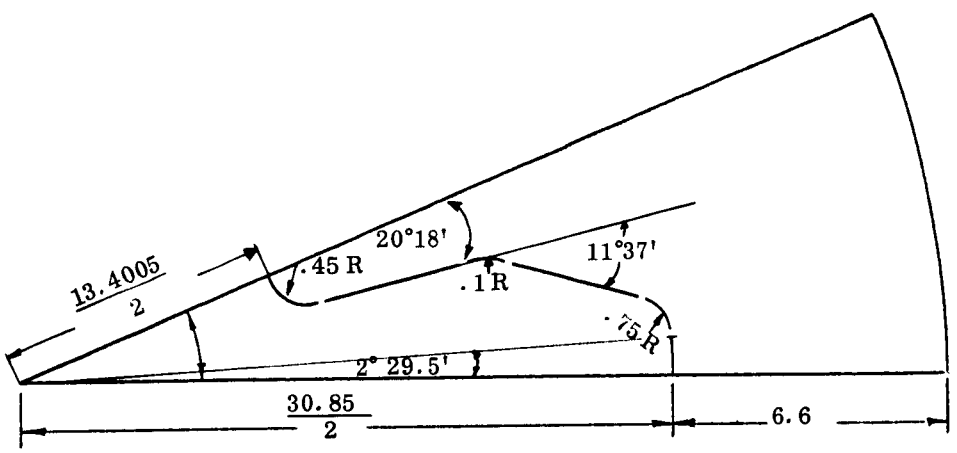

FIGURE 9. SCHEMATIC OF SOLID PROPELLANT ROCKET MOTOR FOR WHICH FULL COMPUTER OUTPUT IS PRESENTED IN TABLES II-XI

GENERALIZED GRAIN DESIGN PROGRAM

GRAIN DESIGN INPUT GENERATOR

COMPLETE SOLID PROPELLANT ROCKET MOTOR EVALUATION TEST CASE

INPUT

CONTROL PARAMETERS

ZNPCT	ZEND	ZRND	ZNCORE
1.0			

CASE PARAMETERS

AC	RC	ZC	DIAM	ACA	RCA	ZCA
22.025	1.4	15.7	44.05	22.025	1.4	

CROSS SECTION PARAMETERS

R1	R2	R3	T1	T3	SN
.45	0.1	0.75	13.4005	30.85	8.0

THET1D	THET1M	THET2D	THET2M	THET3D	THET3M
0.0	18.0	11.0	37.0	2.0	29.5

CASEM	CASECG	PROPD	PORT	AFTCUT	WEB
75.76	-0.66	0.0632	10.0	9.735	6.6

DELX	DELY	DELZ	DELTHD	DELTHM
.3	0.3	0.5	5.0	

TABLE 4. REPRODUCTION OF INPUT DATA TO PROGRAM AGDA FOR ROCKET SHOWN IN FIGURE 2
(Blank spaces indicate zero)

GENERALIZED GRAIN DESIGN PROGRAM

COMPLETE SOLID PROPELLANT ROCKET MOTOR EVALUATION TEST CASE

CHECK OUTPUT AND CORE ROUND CORRECTION

X	Y	Z	R	THETA	(S,Y)	(S,Z)	(S,H)
0.000000	0.000000	24.832141	0.000000	22.5000	90.0000	0.0000	90.0000
0.300000	0.124264	24.829965	0.324718	22.5000	90.0000	0.7676	90.0000
0.600000	0.248528	24.823436	0.649435	22.5000	90.0000	1.5363	90.0000
0.724264	0.300000	24.819454	0.783938	22.5000	90.0000	1.8548	90.0000
0.900000	0.372792	24.812545	0.974153	22.5000	90.0000	2.3059	90.0000
1.200000	0.497056	24.797279	1.298871	22.5000	90.0000	3.0776	90.0000
1.448528	0.600000	24.781366	1.567876	22.5000	90.0000	3.7189	90.0000
1.500000	0.621320	24.777620	1.623588	22.5000	90.0000	3.8519	90.0000
1.800000	0.745584	24.753543	1.948306	22.5000	90.0000	4.6294	90.0000
2.100000	0.869848	24.725020	2.273024	22.5000	90.0000	5.4110	90.0000
2.172792	0.900000	24.717425	2.351813	22.5000	90.0000	5.6013	90.0000
2.400000	0.994113	24.692014	2.597741	22.5000	90.0000	6.1972	90.0000
2.700000	1.118377	24.654485	2.922459	22.5000	90.0000	6.9889	90.0000
2.897056	1.200000	24.627350	3.135751	22.5000	90.0000	7.5122	90.0000
3.000000	1.242641	24.612385	3.247176	22.5000	90.0000	7.7867	90.0000
3.300000	1.366905	24.565657	3.571894	22.5000	90.0000	8.5916	90.0000
3.600000	1.491169	24.514243	3.896612	22.5000	90.0000	9.4042	90.0000
3.621320	1.500000	24.510409	3.919689	22.5000	90.0000	9.4623	90.0000
3.900000	1.615433	24.458071	4.221330	22.5000	90.0000	10.2256	90.0000
4.200000	1.739697	24.397063	4.546047	22.5000	90.0000	11.0566	90.0000
4.345585	1.800000	24.365692	4.703627	22.5000	90.0000	11.4637	90.0000
4.500000	1.863961	24.331139	4.870765	22.5000	90.0000	11.8932	90.0000
4.800000	1.988225	24.260193	5.195482	22.5000	90.0000	12.7516	90.0000
5.069849	2.100000	24.192010	5.487565	22.5000	90.0000	13.5301	90.0000
5.100000	2.112489	24.184130	5.520200	22.5000	90.0000	13.6178	90.0000
5.400000	2.236753	24.102825	5.844918	22.5000	90.0000	14.4981	90.0000
5.700000	2.361017	24.016152	6.169636	22.5000	90.0000	15.3937	90.0000
5.794113	2.400000	23.987831	6.271502	22.5000	90.0000	15.6781	90.0000
6.000000	2.485281	23.923967	6.494353	22.5000	90.0000	16.3061	90.0000
6.190224	2.564077	23.862589	6.700251	22.5000	67.5003	16.8941	73.1059
6.200973	2.540124	23.862342	6.701067	22.2756	64.1570	16.8965	73.1373
6.213159	2.516738	23.861594	6.703530	22.0512	60.7989	16.9035	73.2318
6.226756	2.494008	23.860341	6.707649	21.8276	57.4261	16.9154	73.3899
6.241735	2.472022	23.858581	6.713430	21.6059	54.0383	16.9320	73.6118
6.258063	2.450867	23.856312	6.720871	21.3870	50.6354	16.9535	73.8974
6.275703	2.430629	23.853541	6.729963	21.1718	47.2166	16.9795	74.2463
6.294610	2.411390	23.850258	6.740690	20.9612	43.7816	17.0105	74.6580
6.306948	2.400000	23.847974	6.748154	20.8335	41.6435	17.0321	74.9444
6.313560	2.394236	23.846708	6.752288	20.7678	40.5265	17.0440	75.1036
6.333531	2.378125	23.842719	6.765286	20.5802	37.2590	17.0815	75.6017
6.354496	2.363106	23.838291	6.779667	20.3991	33.9750	17.1236	76.1536

TABLE III. REPRODUCTION OF "TAPE 3" AGDA OUTPUT
(Figures 3 and 4 illustrate meaning of these numbers)

GENERALIZED GRAIN DESIGN PROGRAM

COMPLETE SOLID PROPELLANT ROCKET MOTOR EVALUATION TEST CASE

X	Y	Z	R	THETA	(S,Y)	(H,Z)	(S,H)
6.376430	2.349228	23.833432	6.795420	20.2250	30.6698	17.1686	76.7583
6.399276	2.336561	23.828146	6.812507	20.0586	27.3432	17.2180	77.4144
6.422972	2.325173	23.822445	6.830885	19.9007	23.9954	17.2712	78.1206
6.447448	2.315128	23.816332	6.850504	19.7520	20.6262	17.3281	78.8749
6.472635	2.306491	23.809828	6.871310	19.6133	17.2355	17.3886	79.6755
6.498455	2.299316	23.802949	6.893241	19.4851	13.8230	17.4523	80.5205
6.524826	2.293660	23.795703	6.916230	19.3680	10.3884	17.5194	81.4076
6.551664	2.289572	23.788119	6.940205	19.2627	6.9313	17.5893	82.3344
6.578879	2.287099	23.780214	6.965089	19.1696	3.4515	17.6620	83.2984
6.606375	2.286284	23.772009	6.990800	19.0893	-0.0512	17.7373	84.2968
6.623244	2.286614	23.766868	7.006851	19.0468	-2.1998	17.7844	84.9216
6.923244	2.298138	23.672172	7.294707	18.3633	-2.1998	18.6373	84.8961
7.223244	2.309663	23.572312	7.583522	17.7319	-2.1998	19.5112	84.8689
7.523244	2.321188	23.467124	7.873190	17.1469	-2.1998	20.4075	84.8401
7.823244	2.332713	23.356410	8.163620	16.6034	-2.1998	21.3278	84.8093
8.123244	2.344238	23.239977	8.454735	16.0973	-2.1998	22.2739	84.7757
8.423244	2.355763	23.117592	8.746465	15.6249	-2.1998	23.2479	84.7420
8.723244	2.367287	22.988992	9.038752	15.1831	-2.1998	24.2522	84.7051
8.790053	2.369846	22.959484	9.103912	15.0885	-2.2002	24.4802	84.6968
8.796120	2.369896	22.956809	9.109782	15.0789	1.2763	24.5008	83.2938
8.802218	2.369575	22.954161	9.115587	15.0670	4.7762	24.5212	81.9012
8.810253	2.368580	22.950736	9.123088	15.0478	9.4166	24.5476	80.0930
9.110253	2.318826	22.821029	9.400727	14.2802	9.4166	25.5395	80.0219
9.410253	2.269072	22.684520	9.679956	13.5568	9.4166	26.5690	79.9461
9.710253	2.219317	22.540878	9.960642	12.8741	9.4166	27.6394	79.8653
10.010253	2.169563	22.389695	10.242663	12.2288	9.4166	28.7544	79.7791
10.310253	2.119809	22.230522	10.525915	11.6182	9.4166	29.9135	79.6870
10.429692	2.100000	22.164814	10.639007	11.3842	9.4166	30.3967	79.6485
10.610253	2.070054	22.062839	10.810299	11.0397	9.4166	31.1369	79.5884
10.910253	2.020300	21.886056	11.095730	10.4909	9.4166	32.4158	79.4828
11.210253	1.970546	21.699459	11.382127	9.9696	9.4166	33.7628	79.3695
11.510253	1.920792	21.502233	11.669419	9.4740	9.4166	35.1866	79.2476
11.810253	1.871037	21.293379	11.957543	9.0023	9.4166	36.6984	79.1161
12.110253	1.821283	21.071704	12.246439	8.5527	9.4166	38.3119	78.9738
12.238580	1.800000	20.972610	12.370240	8.3668	9.4166	39.0372	78.9093
12.410253	1.771529	20.835731	12.536055	8.1239	9.4166	40.0441	78.8194
12.710253	1.721774	20.583648	12.826341	7.7145	9.4166	41.9170	78.6511
13.010253	1.672020	20.313044	13.117253	7.3233	9.4166	43.9598	78.4668
13.310253	1.622266	20.020780	13.408749	6.9490	9.4166	46.2119	78.2637
13.610253	1.572511	19.702569	13.700794	6.5907	9.4166	48.7283	78.0382
13.910253	1.522757	19.352159	13.993352	6.2473	9.4166	51.5909	77.7858

TABLE REPRODUCTION OF PAGE 2 OF "TAPE 3" AGDA OUTPUT

GENERALIZED GRAIN DESIGN PROGRAM

COMPLETE SOLID PROPELLANT ROCKET MOTOR EVALUATION TEST CASE

X	Y	Z	R	THETA	(S,Y)	(H,Z)	(S,H)
14.047468	1.500000	19.178724	14.127326	6.0950	9.4166	53.0480	77.6597
14.210253	1.473003	18.959952	14.286392	5.9180	9.4166	54.9280	77.5000
14.510253	1.423248	18.509560	14.579885	5.6020	9.4166	58.9621	77.1716
14.783834	1.377875	18.021092	14.847904	5.3247	9.4166	63.6179	76.8234
14.828248	1.369126	17.931825	14.891320	5.2753	12.8753	64.5032	73.6635
14.872167	1.357677	17.840472	14.934009	5.2161	16.3431	65.4207	70.4782
14.915425	1.343554	17.747043	14.975814	5.1472	19.8200	66.3712	67.2500
14.957859	1.326786	17.651610	15.016587	5.0690	23.3062	67.3550	63.9851
14.999306	1.307408	17.554289	15.056177	4.9816	26.8020	68.3718	60.6838
15.039606	1.285478	17.455135	15.094442	4.8854	30.3076	69.4218	57.3465
15.078603	1.261048	17.354268	15.131242	4.7806	33.8236	70.5046	53.9730
15.116142	1.234188	17.251702	15.166441	4.6677	37.3504	71.6207	50.5636
15.152073	1.204966	17.147496	15.199909	4.5469	40.9891	72.7701	47.1178
15.157753	1.200000	17.130406	15.205179	4.5265	41.4655	72.9600	46.5542
15.186250	1.173473	17.041721	15.231520	4.4186	44.4400	73.9524	43.6357
15.218533	1.139780	16.934473	15.261154	4.2831	48.0054	75.1668	40.1153
15.247043	1.106174	16.832222	15.287116	4.1495	51.3725	76.3390	36.7720
15.273603	1.070854	16.728827	15.311095	4.0105	54.7490	77.5379	33.3994
15.298086	1.033945	16.624559	15.332986	3.8665	58.1331	78.7600	30.0018
15.320389	0.995584	16.519368	15.352703	3.7181	61.5234	80.0054	26.5813
15.340396	0.955933	16.413635	15.370150	3.5658	64.9168	81.2683	23.1432
15.357996	0.915242	16.307463	15.385242	3.4104	68.3041	82.5481	19.6974
15.363869	0.900000	16.268152	15.390206	3.3525	69.5520	83.0242	18.4245
15.373234	0.873366	16.200389	15.398021	3.2515	71.7089	83.8476	16.2224
15.386031	0.830378	16.092272	15.408421	3.0892	75.1359	85.1679	12.7148
15.396291	0.786414	15.982956	15.416361	2.9240	78.5853	86.5094	9.1753
15.403937	0.741617	15.872899	15.421778	2.7564	82.0575	87.8650	5.6072
15.408868	0.696139	15.762443	15.424584	2.5867	85.5527	89.2285	2.0140
15.410416	0.670597	15.707111	15.424999	2.4917	87.5083	89.9121	0.0869
15.413326	0.600000	15.707111	15.424999	2.2292	87.7707	89.9121	0.0869
15.422082	0.300000	15.707111	15.424999	1.1144	88.8856	89.9121	0.0869
15.423409	0.221540	15.707111	15.424999	0.8229	89.1771	89.9121	0.0850
15.425000	0.000000	15.707111	15.424999	0.0000	90.0000	89.9121	0.0888

TABLE REPRODUCTION OF PAGE 3 OF AGDA COMPUTER OUTPUT

GENERALIZED GRAIN DESIGN PROGRAM

COMPLETE SOLID PROPELLANT ROCKET MOTOR EVALUATION TEST CASE

SUPPLEMENTARY CHECK RESULTS

	TOTAL	HEAD END	TOP SECT. ST. THRU	CENTER SECT. ST. THRU	AFT END
SURFACE	4022.39	509.56	878.05	2634.79	0.00
VOLUME	9434.28		2899.71	6534.57	0.00

PORT AREA = 416.0262

TABLE VI. CHECK RESULTS
(These results are based only upon "Tape 3" data and therefore serve to validate the majority of AGDA.)

COMPUTED TRACE OF INTERNAL GEOMETRY

COMPLETE SOLID PROPELLANT ROCKET MOTOR EVALUATION TEST CASE

WEB BURNOUT (PERCENT)	CHAMBER SURFACE (SQ-IN)	CHAMBER VOLUME (CU-IN)	FIRST Z MOMENT (IN**4)
0	5.5747E 03	1.7151E 04	3.8688E 05
5	5.7019E 03	1.9012E 04	3.7302E 05
10	5.6624E 03	2.0901E 04	3.5862E 05
15	5.5267E 03	2.2747E 04	3.4420E 05
20	5.4046E 03	2.4546E 04	3.2976E 05
25	5.4202E 03	2.6331E 04	3.1509E 05
30	5.4407E 03	2.8123E 04	3.0001E 05
35	5.4533E 03	2.9920E 04	2.8449E 05
40	5.4620E 03	3.1720E 04	2.6850E 05
45	5.4666E 03	3.3522E 04	2.5201E 05
50	5.4663E 03	3.5325E 04	2.3499E 05
55	5.4621E 03	3.7127E 04	2.1741E 05
60	5.4524E 03	3.8926E 04	1.9921E 05
65	5.4373E 03	4.0722E 04	1.8039E 05
70	5.4150E 03	4.2511E 04	1.6089E 05
75	5.3858E 03	4.4292E 04	1.4066E 05
80	5.3518E 03	4.6060E 04	1.1971E 05
85	5.3232E 03	4.7818E 04	9.7932E 04
90	5.3015E 03	4.9568E 04	7.5305E 04
95	5.2695E 03	5.1309E 04	5.1799E 04
100-	5.2273E 03		
100+	4.4455E 03	5.3027E 04	2.7563E 04
105	2.4510E 03	5.4002E 04	1.7304E 04
110	1.8014E 03	5.4692E 04	1.0595E 04
115	1.2943E 03	5.5193E 04	5.9546E 03
120	8.7868E 02	5.5546E 04	2.8386E 03
125	5.0963E 02	5.5771E 04	9.6954E 02
130	1.6718E 02	5.5878E 04	1.2255E 02

WEB THICKNESS =	6.600
HEIGHT =	15.700
DIAMETER =	44.050
CASE VOLUME =	55894.089
INHIBITED PORT DIAMETER =	10.000

TABLE VII. FIRST PAGE OF ORIGINAL PROGRAM AGDA OUTPUT

COMPUTED TRACE OF MOMENTS OF INERTIA

COMPLETE SOLID PROPELLANT ROCKET MOTOR EVALUATION TEST CASE

WEB BURNOUT (PERCENT)	I-XX (IN**5)	I-YY (IN**5)	I-ZZ (IN**5)
0	1.3464E 07	1.3464E 07	1.0534E 07
5	1.3054E 07	1.3054E 07	1.0280E 07
10	1.2619E 07	1.2619E 07	1.0000E 07
15	1.2171E 07	1.2171E 07	9.7007E 06
20	1.1710E 07	1.1710E 07	9.3811E 06
25	1.1230E 07	1.1230E 07	9.0394E 06
30	1.0726E 07	1.0726E 07	8.6734E 06
35	1.0199E 07	1.0199E 07	8.2833E 06
40	9.6484E 06	9.6484E 06	7.8691E 06
45	9.0732E 06	9.0732E 06	7.4313E 06
50	8.4736E 06	8.4736E 06	6.9701E 06
55	7.8491E 06	7.8491E 06	6.4859E 06
60	7.1994E 06	7.1994E 06	5.9794E 06
65	6.5245E 06	6.5245E 06	5.4513E 06
70	5.8240E 06	5.8240E 06	4.9026E 06
75	5.0975E 06	5.0975E 06	4.3345E 06
80	4.3465E 06	4.3465E 06	3.7491E 06
85	3.5690E 06	3.5690E 06	3.1464E 06
90	2.7642E 06	2.7642E 06	2.5266E 06
95	1.9318E 06	1.9318E 06	1.8905E 06
100	1.0789E 06	1.0789E 06	1.2447E 06
105	6.8974E 05	6.8974E 05	8.3811E 05
110	4.2827E 05	4.2827E 05	5.4197E 05
115	2.4406E 05	2.4406E 05	3.2124E 05
120	1.1819E 05	1.1819E 05	1.6209E 05
125	4.0706E 04	4.0706E 04	5.8056E 04
130	4.0489E 02	6.3055E 01	8.5904E 01

TABLE VIII. PAGE 2 OF ORIGINAL PROGRAM AGDA OUTPUT

COMPUTED TRACE OF PRODUCTS OF INERTIA

COMPLETE SOLID PROPELLANT ROCKET MOTOR EVALUATION TEST CASE

WEB BURNOUT (PERCENT)	I-XY (IN**5)	I-XZ (IN**5)	I-YZ (IN**5)
0	8.2441E-02	3.4223E-02	1.2320E-01
5	8.0341E-02	3.3352E-02	1.2007E-01
10	7.8064E-02	3.2414E-02	1.1669E-01
15	7.5633E-02	3.1432E-02	1.1315E-01
20	7.3051E-02	3.0408E-02	1.0947E-01
25	7.0301E-02	2.9330E-02	1.0559E-01
30	6.7370E-02	2.8191E-02	1.0149E-01
35	6.4259E-02	2.6986E-02	9.7150E-02
40	6.0969E-02	2.5711E-02	9.2559E-02
45	5.7502E-02	2.4362E-02	8.7703E-02
50	5.3861E-02	2.2935E-02	8.2567E-02
55	5.0046E-02	2.1427E-02	7.7137E-02
60	4.6062E-02	1.9832E-02	7.1396E-02
65	4.1912E-02	1.8147E-02	6.5329E-02
70	3.7603E-02	1.6366E-02	5.8917E-02
75	3.3140E-02	1.4483E-02	5.2138E-02
80	2.8538E-02	1.2494E-02	4.4979E-02
85	2.3797E-02	1.0390E-02	3.7403E-02
90	1.8918E-02	8.1636E-03	2.9389E-02
95	1.3912E-02	5.8095E-03	2.0914E-02
100	8.8328E-03	3.3369E-03	1.2013E-02
105	5.8069E-03	2.1241E-03	7.6468E-03
110	3.6828E-03	1.3135E-03	4.7287E-03
115	2.1436E-03	7.4426E-04	2.6793E-03
120	1.0637E-03	3.5736E-04	1.2865E-03
125	3.7522E-04	1.2278E-04	4.4201E-04
130	0.0000E 00	1.5602E 02	0.0000E 00

TABLE IX. PAGE 3 OF ORIGINAL PROGRAM AGDA OUTPUT

THIOKOL-ELKTON
ADVANCED GRAIN DESIGN COMPUTER PROGRAM

COMPLETE SOLID PROPELLANT ROCKET MOTOR EVALUATION TEST CASE

THEORETICAL ANALYSIS BY F.E.MOORE
PROGRAMMING ANALYSIS BY D.H.FREDERICK

WEB BURN PCT	BURNING SURFACE (SQ-IN)	CHAMBER VOLUME (CU-IN)	PROP. VOLUME (CU-IN)	PROP. CG (IN)	PROPELLANT INERTIA TENSOR I-XX (SQ-FT*CU-IN)	I-YY	I-ZZ
0	5574.66	17151.03	38743.06	9.986	93500.6	93500.6	73154.8
5	5701.89	19011.64	36882.45	10.114	90655.6	90655.6	71385.5
10	5662.43	20901.43	34992.66	10.248	87634.9	87634.9	69447.8
15	5526.67	22747.39	33146.70	10.384	84521.2	84521.2	67365.9
20	5404.55	24546.06	31348.03	10.519	81318.8	81318.8	65146.9
25	5420.16	26330.97	29563.12	10.658	77984.9	77984.9	62773.9
30	5440.68	28122.73	27771.36	10.803	74488.9	74488.9	60232.1
35	5453.31	29919.56	25974.53	10.953	70828.9	70828.9	57522.7
40	5461.95	31719.94	24174.15	11.107	67002.6	67002.6	54646.6
45	5466.61	33522.22	22371.87	11.265	63008.6	63008.6	51606.0
50	5466.34	35324.93	20569.16	11.425	58844.7	58844.7	48403.2
55	5462.09	37126.86	18767.23	11.584	54508.0	54508.0	45040.8
60	5452.42	38926.37	16967.72	11.741	49996.1	49996.1	41523.6
65	5437.26	40721.74	15172.35	11.889	45308.7	45308.7	37856.2
70	5415.02	42510.87	13383.22	12.021	40444.2	40444.2	34046.0
75	5385.84	44291.97	11602.12	12.124	35399.6	35399.6	30100.9
80	5351.81	46059.71	9834.38	12.173	30184.3	30184.3	26035.4
85	5323.25	47817.55	8076.54	12.126	24784.6	24784.6	21850.3
90	5301.46	49567.61	6326.48	11.903	19195.9	19195.9	17545.6
95	5269.46	51309.21	4584.88	11.298	13415.4	13415.4	13128.6
100	5227.27	53026.60	2867.49	9.612	7492.2	7492.2	8644.1
MAX	5701.89	53026.60	38743.06	12.173	93500.6	93500.6	73154.8
MIN	5227.27	17151.03	2867.49	9.612	7492.2	7492.2	8644.1
AVG	5438.34	35269.35	20624.73	11.140	55739.0	55739.0	45593.2
100+	4445.55						
105	2450.99	54001.86	1892.23		4789.8	4789.8	5820.2
110	1801.36	54691.78	1202.31		2974.1	2974.1	3763.7
115	1294.28	55192.89	701.20		1694.9	1694.9	2230.8
120	878.68	55545.79	348.30		820.8	820.8	1125.6
125	509.63	55771.24	122.85		282.7	282.7	403.2
130	167.18	55878.48	15.61		2.8	0.4	0.6

PER CENT PROPELLANT (0-100 PCT WEB) BY VOLUME = 64.18

PER CENT PROPELLANT (100-130 PCT WEB) BY VOLUME = 5.13

TABLE X. PAGE 1 OF NEW PROGRAM AGDA OUTPUT

(The max., min., and average values refer only to O→100 pct web.
The 100 + surface area is the surface just after web burnout.)

THIOKOL-ELKTON
ADVANCED GRAIN DESIGN COMPUTER PROGRAM

COMPLETE SOLID PROPELLANT ROCKET MOTOR EVALUATION TEST CASE

THEORETICAL ANALYSIS BY F.E.MOORE
PROGRAMMING ANALYSIS BY D.H.FREDERICK

WEB BURN	BURNING SURFACE	PROP. WEIGHT	SYSTEM WEIGHT	SYSTEM CG	PROPELLANT INERTIA TENSOR I-XX	I-YY	I-ZZ
PCT	(SQ-IN)	(LBS)	(LBS)	(IN)	--------(SQ-FT*LBS)--------		
0	5574.66	2448.56	3154.32	7.604	5909.2	5909.2	4623.4
5	5701.89	2330.97	3036.73	7.610	5729.4	5729.4	4511.6
10	5662.43	2211.54	2917.30	7.609	5538.5	5538.5	4389.1
15	5526.67	2094.87	2800.63	7.601	5341.7	5341.7	4257.5
20	5404.55	1981.20	2686.96	7.583	5139.3	5139.3	4117.3
25	5420.16	1868.39	2574.15	7.555	4928.6	4928.6	3967.3
30	5440.68	1755.15	2460.91	7.515	4707.7	4707.7	3806.7
35	5453.31	1641.59	2347.35	7.461	4476.4	4476.4	3635.4
40	5461.95	1527.81	2233.57	7.389	4234.6	4234.6	3453.7
45	5466.61	1413.90	2119.66	7.294	3982.1	3982.1	3261.5
50	5466.34	1299.97	2005.73	7.172	3719.0	3719.0	3059.1
55	5462.09	1186.09	1891.85	7.017	3444.9	3444.9	2846.6
60	5452.42	1072.36	1778.12	6.819	3159.8	3159.8	2624.3
65	5437.26	958.89	1664.65	6.569	2863.5	2863.5	2392.5
70	5415.02	845.82	1551.58	6.253	2556.1	2556.1	2151.7
75	5385.84	733.25	1439.01	5.854	2237.3	2237.3	1902.4
80	5351.81	621.53	1327.29	5.349	1907.6	1907.6	1645.4
85	5323.25	510.44	1216.20	4.706	1566.4	1566.4	1380.9
90	5301.46	399.83	1105.59	3.883	1213.2	1213.2	1108.9
95	5269.46	289.76	995.52	2.820	847.9	847.9	829.7
100	5227.27	181.23	886.99	1.439	473.5	473.5	546.3
MAX	5701.89	2448.56	3154.32	7.610	5909.2	5909.2	4623.4
MIN	5227.27	181.23	886.99	1.439	473.5	473.5	546.3
AVG	5438.34	1303.48	2009.24	6.338	3522.7	3522.7	2881.5
100+	4445.55						
105	2450.99	119.59	825.35	0.761	302.7	302.7	367.8
110	1801.36	75.99	781.75	0.261	188.0	188.0	237.9
115	1294.28	44.32	750.08	-0.119	107.1	107.1	141.0
120	878.68	22.01	727.77	-0.394	51.9	51.9	71.1
125	509.63	7.76	713.52	-0.567	17.9	17.9	25.5
130	167.18	0.99	706.75	-0.648	0.2	0.0	0.0

TABLE XI. PAGE 2 OF NEW PROGRAM AGDA FINAL OUTPUT

(This page includes the weight of inert parts as well as propellant density to obtain actual weight, CG travel, etc.)

of the rocket motor core. These coordinates are defined by the intersection of the side of a star point and the core head. Figures 10 and 11 illustrate the area just described.

At the conclusion of the Tape 3 output, the supplementary check results are printed (Table VI). These results are obtained from Tape 3 data only, and no use is made of the bulk of the Advanced Grain Design Analysis program. Initial surface area and initial chamber volume are calculated.

The next three pages of output (Tables VII, VIII, and IX) are in the original output format. Table VI shows burning surface, chamber volume, and the first moment of the propellant along the Z axis. Table VIII shows the moments of inertia, while Table IX shows the products of inertia.

The final two pages of computer output (Tables X and XI) represent the new output data format. These pages are identical except for the fact that Table X is independent of propellant density, while Table XI utilizes this quantity for determination of propellant weight, etc. Case weight and payload weight, if specified to the program, are used in conjunction with the computed propellant center of gravity travel to compute the C. G. travel of the entire system.

The three-dimensional AGDA computer program appears to operate properly for all test cases evaluated. Reservation is implied here since the rigorous analysis of the AGDA is unmatched by manual analysis and other known computer analyses. Accordingly, minor differences between predicted and AGDA determined answers cannot be readily resolved. Despite its complexity, the program is extremely easy to use. The input data generator has all but eliminated errors caused by incorrect input data. In addition

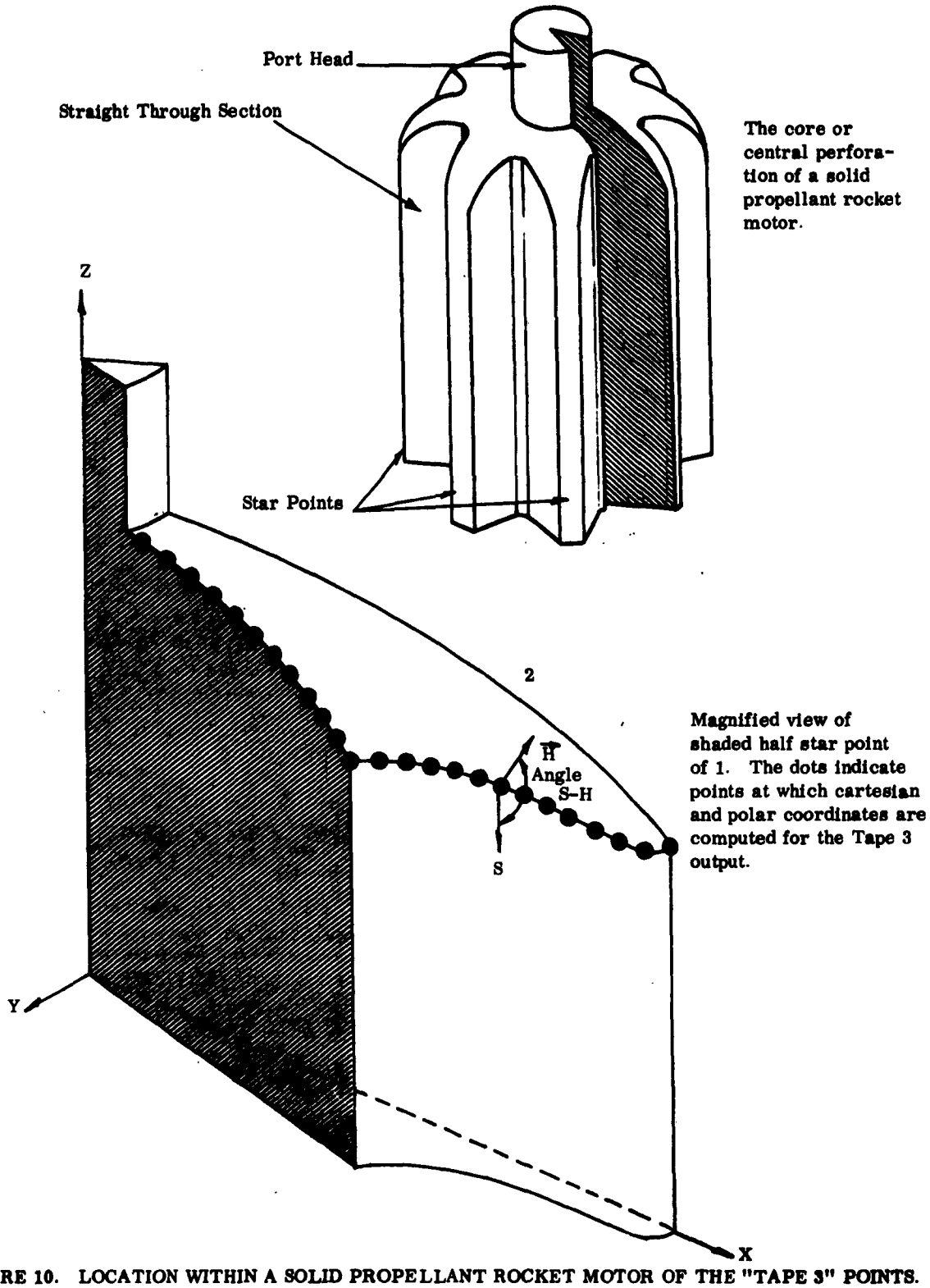

FIGURE 10. LOCATION WITHIN A SOLID PROPELLANT ROCKET MOTOR OF THE "TAPE 3" POINTS.

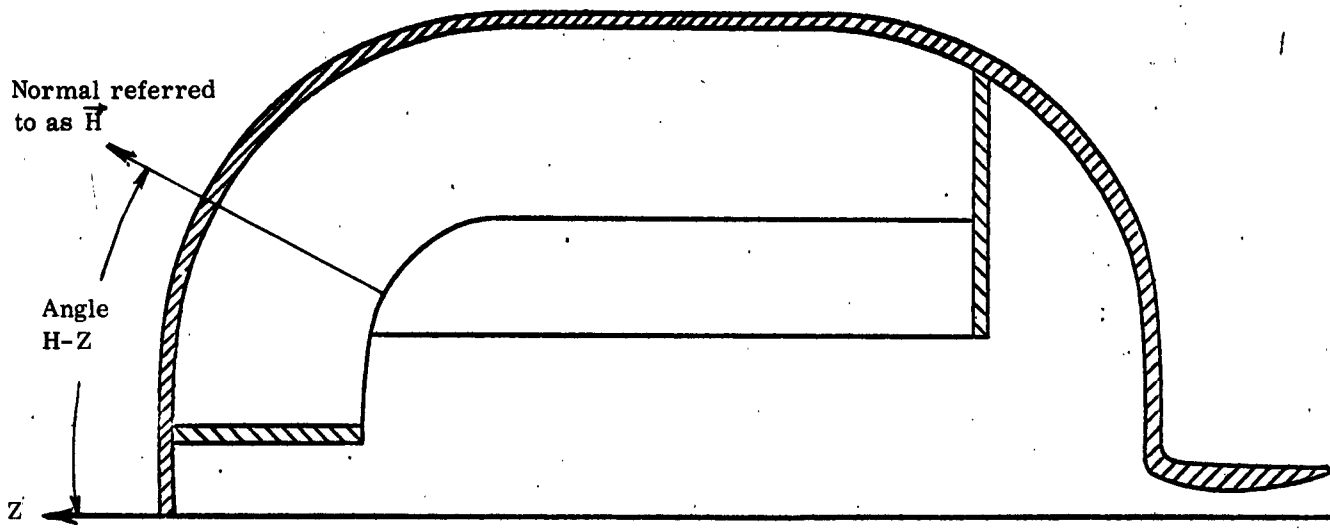

Longitudinal cross section of rocket motor which reveals the normal $\vec{H}$ and the angle Z-H

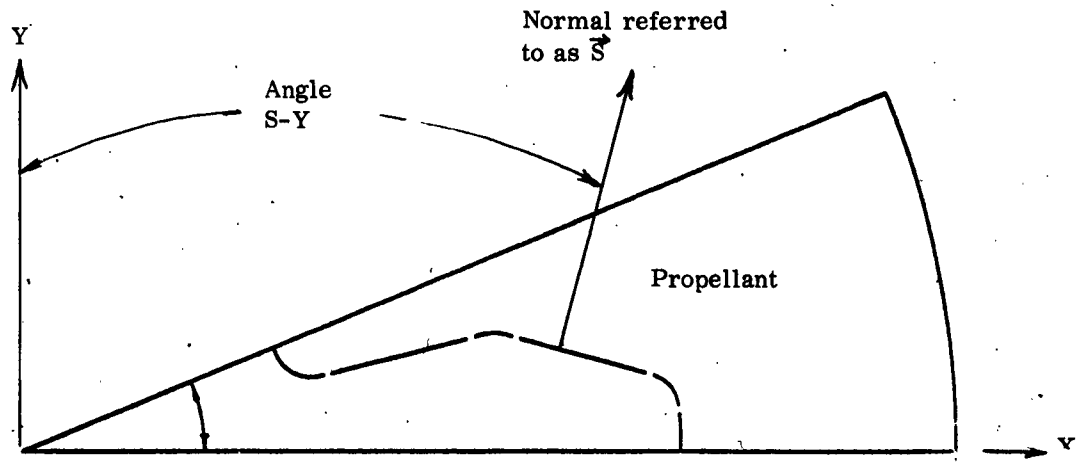

Axial cross section of one half star point which reveals the normal $\vec{S}$ and the angle S-Y

The angle S-H is simply the angle between normals $\vec{H}$ and $\vec{S}$. Reference back to Figure 10 will show a three dimensional illustration of both $\vec{S}$ and $\vec{H}$ and the angle S-H.

FIGURE 11. DEFINITION OF NORMALS $\vec{S}$ AND $\vec{H}$ TOGETHER WITH THEIR ASSOCIATED ANGLES.

to an easily readable format, the AGDA output provides check results that may be compared to the main program output for the purpose of checking program accuracy.

C. Irregular Temperature Profile

The straight-through portion of the AGDA computer program was modified according to the theory presented in the previous quarterly report[1] in order to analyze solid propellant rocket motors having a variable grain temperature profile. At the present time, these modifications permit temperature variation over only one half star point of the rocket motor. Test results for debugging purposes may be obtained in a much shorter period of time when only one half star point is analyzed. Although in principle an entire rocket motor can be analyzed by manually executing one half star point at a time, the capability of automatically performing the complete analysis will be included once the program is fully checked out for the half star point case.

Three test cases have been run with the present version of the variable temperature program. Each test case involved the straight-through section of the rocket motor shown in Figure 9.

Case I - Constant temperature -- Variable temperature option disabled

Case II - Constant temperature -- Variable temperature option used with table of equal temperature

Case III - Variable temperature option used with nonuniform grain temperature.

Inspection of Tables XII and XIII, which are reproductions of the final page of output from test case I and test case II, respectively, shows that these outputs are identical. This is the desired result.

THIOKOL-ELKTON
ADVANCED GRAIN DESIGN COMPUTER PROGRAM

STRAIGHT THRU SECTION BROKEN BACK STAR VARIABLE TEMP OPTION DISABLED

THEORETICAL ANALYSIS BY F.E.MOORE
PROGRAMMING ANALYSIS BY D.H.FREDERICK

WEB BURN	BURNING SURFACE	CHAMBER VOLUME	PROP. VOLUME	PROP. CG	PROPELLANT INERTIA TENSOR I-XX	I-YY	I-ZZ
PCT	(SQ-IN)	(CU-IN)	(CU-IN)	(IN)	------(SQ-FT*CU-IN)------		
0	2634.05	6556.54	17370.08	7.850	28072.6	28072.6	36323.3
5	2666.59	7430.92	16495.70	7.850	27138.3	27138.3	35452.4
10	2620.76	8310.01	15616.61	7.850	26163.4	26163.4	34505.8
15	2530.06	9159.67	14766.95	7.850	25173.5	25173.5	33495.6
20	2445.54	9978.20	13948.42	7.850	24171.6	24171.6	32425.8
25	2426.25	10781.46	13145.16	7.850	23145.0	23145.1	31289.4
30	2409.74	11579.18	12347.44	7.850	22085.2	22085.2	30080.0
35	2393.22	12371.46	11555.16	7.850	20991.5	20991.5	28796.8
40	2376.71	13158.30	10768.33	7.850	19863.8	19863.8	27439.3
45	2360.20	13939.68	9986.94	7.850	18701.9	18701.9	26007.2
50	2343.68	14715.61	9211.01	7.850	17505.7	17505.7	24500.3
55	2327.17	15486.10	8440.52	7.850	16275.3	16275.3	22918.7
60	2310.65	16251.14	7675.48	7.850	15010.8	15010.8	21262.7
65	2294.14	17010.73	6915.89	7.850	13712.4	13712.4	19532.7
70	2277.62	17764.87	6161.75	7.850	12380.5	12380.5	17729.5
75	2261.11	18513.56	5413.06	7.850	11015.4	11015.4	15853.7
80	2247.56	19256.12	4670.51	7.850	9618.9	9618.9	13908.0
85	2243.14	19995.82	3930.80	7.850	8186.2	8186.2	11886.7
90	2248.46	20735.90	3190.72	7.850	6712.1	6712.1	9783.1
95	2260.42	21478.62	2448.00	7.850	5192.4	5192.4	7591.2
100	2279.00	22225.26	1701.36	7.850	3624.2	3624.2	5306.9
MAX	2666.59	22225.26	17370.08	7.850	28072.6	28072.6	36323.3
MIN	2243.14	6556.54	1701.36	7.850	3624.2	3624.2	5306.9
AVG	2378.86	14604.72	9321.90	7.850	16892.4	16892.4	23147.1
100+	2276.10						
105	1350.28	22743.75	1182.87		2535.6	2535.6	3721.3
110	1052.03	23136.73	789.89		1706.1	1706.1	2510.8
115	803.97	23438.12	488.51		1063.3	1063.3	1569.1
120	584.86	23666.32	260.30		571.3	571.3	845.6
125	375.92	23821.76	104.86		232.1	232.1	344.5
130	157.53	23908.10	18.52		3.3	0.5	0.7

PER CENT PROPELLANT (0-100 PCT WEB) BY VOLUME = 65.49

PER CENT PROPELLANT (100-130 PCT WEB) BY VOLUME = 7.11

TABLE XII. FINAL PAGE OF OUTPUT, TEST CASE 1

THIOKOL-ELKTON
ADVANCED GRAIN DESIGN COMPUTER PROGRAM

Straight Thru Section Broken Back Star Variable Temp Option Employed to Read Table of Const Grain Temp
THEORETICAL ANALYSIS BY F.E.MOORE
PROGRAMMING ANALYSIS BY D.H.FREDERICK

WEB BURN	BURNING SURFACE	CHAMBER VOLUME	PROP. VOLUME	PROP. CG	PROPELLANT INERTIA TENSOR I-XX	I-YY	I-ZZ
PCT	(SQ-IN)	(CU-IN)	(CU-IN)	(IN)	------(SQ-FT*CU-IN)------		
0	2634.05	6556.54	17370.08	7.850	28072.6	28072.6	36323.3
5	2666.59	7430.92	16495.70	7.850	27138.3	27138.3	35452.4
10	2620.76	8310.01	15616.61	7.850	26163.4	26163.4	34505.8
15	2530.06	9159.67	14766.95	7.850	25173.5	25173.5	33495.6
20	2445.54	9978.20	13948.42	7.850	24171.6	24171.6	32425.8
25	2426.25	10781.46	13145.16	7.850	23145.0	23145.1	31289.4
30	2409.74	11579.18	12347.44	7.850	22085.2	22085.2	30080.0
35	2393.22	12371.46	11555.16	7.850	20991.5	20991.5	28796.8
40	2376.71	13158.30	10768.33	7.850	19863.8	19863.8	27439.3
45	2360.20	13939.68	9986.94	7.850	18701.9	18701.9	26007.2
50	2343.68	14715.61	9211.01	7.850	17505.7	17505.7	24500.3
55	2327.17	15486.10	8440.52	7.850	16275.3	16275.3	22918.7
60	2310.65	16251.14	7675.48	7.850	15010.8	15010.8	21262.7
65	2294.14	17010.73	6915.89	7.850	13712.4	13712.4	19532.7
70	2277.62	17764.87	6161.75	7.850	12380.5	12380.5	17729.5
75	2261.11	18513.56	5413.06	7.850	11015.4	11015.4	15853.7
80	2247.56	19256.12	4670.51	7.850	9618.9	9618.9	13908.0
85	2243.14	19995.82	3930.80	7.850	8186.2	8186.2	11886.7
90	2248.46	20735.90	3190.72	7.850	6712.1	6712.1	9783.1
95	2260.42	21478.62	2448.00	7.850	5192.4	5192.4	7591.2
100	2279.00	22225.26	1701.36	7.850	3624.2	3624.2	5306.9
MAX	2666.59	22225.26	17370.08	7.850	28072.6	28072.6	36323.3
MIN	2243.14	6556.54	1701.36	7.850	3624.2	3624.2	5306.9
AVG	2378.86	14604.72	9321.90	7.850	16892.4	16892.4	23147.1
100+	2276.10						
105	1350.28	22743.75	1182.87		2535.6	2535.6	3721.3
110	1052.03	23136.73	789.89		1706.1	1706.1	2510.8
115	803.97	23438.12	488.51		1063.3	1063.3	1569.1
120	584.86	23666.32	260.30		571.3	571.3	845.6
125	375.92	23821.76	104.86		232.1	232.1	344.5
130	157.53	23908.10	18.52		3.3	0.5	0.7

PER CENT PROPELLANT (0-100 PCT WEB) BY VOLUME = 65.49

PER CENT PROPELLANT (100-130 PCT WEB) BY VOLUME = 7.11

TABLE XIII. FINAL PAGE OF OUTPUT, TEST CASE 2

As a further check on the accuracy of the program, a graphical solution of these test cases (uniform grain temperature) was performed. Figure 12 illustrates a comparison of these solutions.

The variable temperature test case used the temperature profile shown in Figure 13. This motor was evaluated by both graphical and computer techniques and the results are also shown in Figure 12. Table XIV is a reproduction of the computer output.

The variation between the computer-derived and graphically-derived solutions is greater for the variable temperature test case than the uniform temperature test case as expected. The principal reason for this is that any small errors occurring in the graphical analysis of the variable temperature test case are cumulative, while those occurring in the constant temperature test case are not cumulative.

The conclusion of maximum importance to be reached by comparison of these analyses is that both graphical and computer solutions follow the same general trend and hence tend to substantiate one another. Further, the departure of the two derived results is relatively small and well within the errors that are anticipated. The effects of a two-dimensional variation in grain temperature may now be analyzed by the Advanced Grain Design Computer Program.

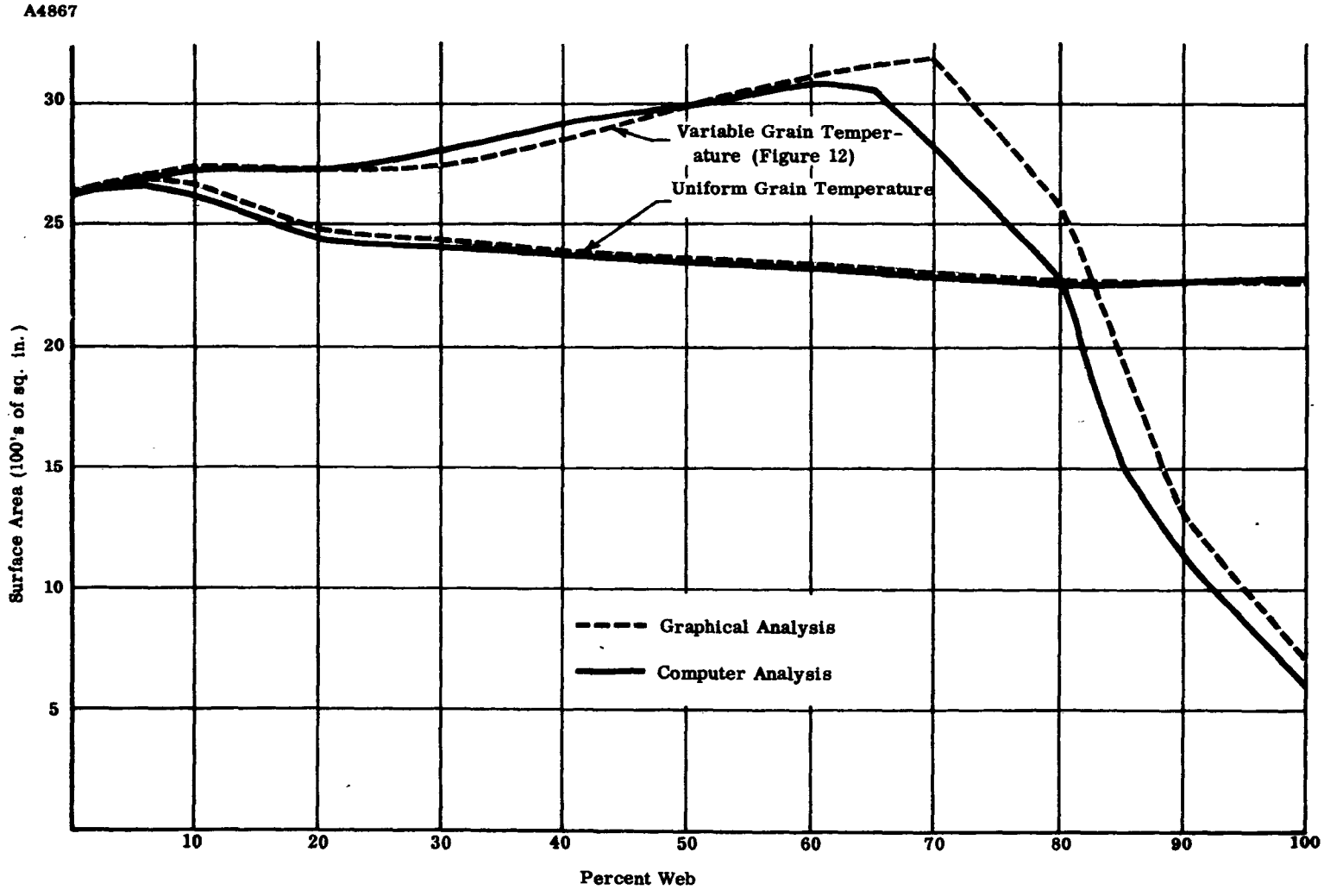

FIGURE 12. COMPARISON OF SOLUTIONS, GRAIN TEMPERATURE TEST CASES

A-4899

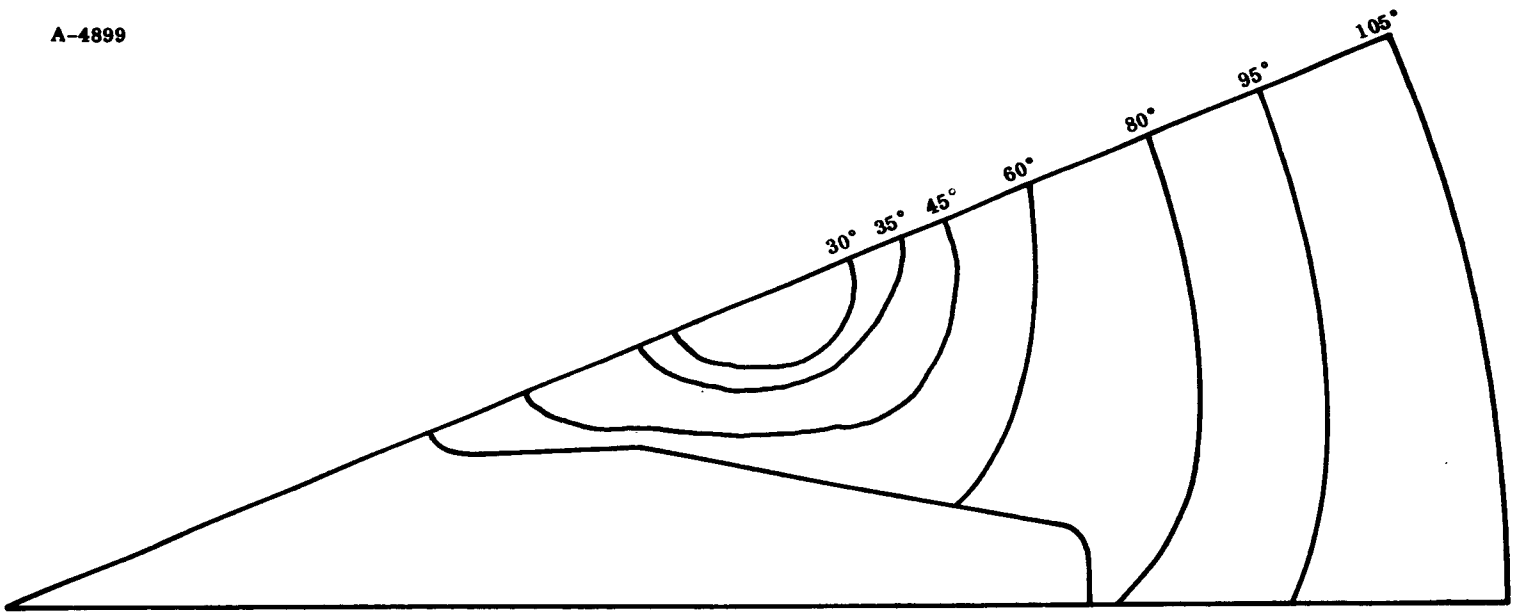

FIGURE 13. GRAIN TEMPERATURE PROFILE USED IN THE VARIABLE TEMPERATURE TEST CASE

THIOKOL-ELKTON
ADVANCED GRAIN DESIGN COMPUTER PROGRAM

Straight Thru Section Broken Back Star Variable Temp Option Employed With Grain Temp Shown in Figure 13
THEORETICAL ANALYSIS BY F.E.MOORE
PROGRAMMING ANALYSIS BY D.H.FREDERICK

WEB BURN	BURNING SURFACE	CHAMBER VOLUME	PROP. VOLUME	PROP. CG	PROPELLANT INERTIA TENSOR I-XX	I-YY	I-ZZ
PCT	(SQ-IN)	(CU-IN)	(CU-IN)	(IN)	------(SQ-FT*CU-IN)------		
0	2634.05	6555.75	17370.87	7.850	27254.5	27254.5	34686.2
5	2690.68	7314.03	16612.59	7.850	26418.0	26418.0	33878.5
10	2728.19	8090.19	15836.43	7.850	25529.7	25529.7	32987.5
15	2737.88	8864.80	15061.82	7.850	24603.9	24603.9	32019.9
20	2698.69	9646.74	14279.88	7.850	23625.4	23625.4	30955.3
25	2711.24	10437.38	13489.24	7.850	22590.5	22590.5	29787.6
30	2794.84	11239.82	12686.80	7.850	21500.9	21500.9	28524.2
35	2856.82	12084.50	11842.12	7.850	20322.6	20322.6	27131.5
40	2904.70	12976.34	10950.28	7.850	19036.4	19036.4	25576.8
45	2945.73	13914.81	10011.82	7.850	17641.5	17641.5	23857.9
50	2995.13	14895.57	9031.05	7.850	16138.2	16138.2	21970.5
55	3034.35	15930.37	7996.25	7.850	14503.6	14503.6	19882.3
60	3078.53	17011.65	6914.97	7.850	12740.9	12740.9	17590.8
65	3057.88	18150.32	5776.30	7.850	10833.7	10833.7	15075.8
70	2812.41	19301.47	4625.15	7.850	8832.5	8832.5	12387.1
75	2557.47	20403.53	3523.09	7.850	6822.3	6822.3	9624.3
80	2298.65	21461.11	2465.51	7.850	4812.5	4812.5	6811.6
85	1517.49	22270.76	1655.86	7.850	3257.3	3257.3	4625.0
90	1151.91	22844.63	1082.00	7.850	2147.5	2147.5	3060.2
95	854.19	23278.67	647.95	7.850	1298.0	1298.0	1856.6
100	624.34	23595.26	331.36	7.850	669.9	669.9	961.7
MAX	3078.53	23595.26	17370.87	7.850	27254.5	27254.5	34686.2
MIN	624.34	6555.75	331.36	7.850	669.9	669.9	961.7
AVG	2461.20	15250.84	8675.77	7.850	14789.5	14789.5	19678.6
100+	606.85						
105	377.39	23811.58	115.04		234.5	234.5	337.8
110	103.60	23916.80	9.82		20.1	20.1	29.1
115	0.00	23926.62	0.00		0.0	0.0	0.0
120	0.00	23926.62	0.00		0.0	0.0	0.0
125	0.00	23926.62	0.00		0.0	0.0	0.0
130	0.00	23926.62	0.00		0.0	0.0	0.0

PER CENT PROPELLANT (0-100 PCT WEB) BY VOLUME = 71.22

PER CENT PROPELLANT (100-130 PCT WEB) BY VOLUME = 1.38

TABLE XIV. COMPUTER OUTPUT FOR VARIABLE TEMPERATURE TEST CASE

III. EFFECT OF STRAIN ON BURNING RATE

Results presented in the previous quarterly progress report[1] indicated that the determination of the effects of volumetric changes (Poisson's ratio) on linear and mass burning rate provided a promising approach to correlating strain effects on burning. During the previous quarter, it was shown that strain per se does not directly influence linear burning rate but may affect other material properties that can be directly related to burning rate changes. The change in volume with strain, also referred to as "Poisson's ratio," is this property. During this quarter, several propellants were investigated by determining the effect of strain on Poisson's ratio and then relating that parameter to any changes in burning rate. On this basis, a criterion for this type of phenomenon may be established based on change in density with strain, whereby one could predict the effect of strain on burning rate by an examination of Poisson's ratio at that strain.

A. Poisson's Ratio

When a material is stretched, cross sectional area changes as well as length. Poisson's ratio, ν, is the parameter relating these changes in dimension and is defined here as:

$$\nu = \frac{\text{Percent change in width}}{\text{Percent change in length}} = \frac{\Delta W/W_o}{\Delta L/L_o} \qquad (1.1)$$

It can be shown that if the volume of a material remains constant when subjected to very small strains, ν is a constant and equals 0.50. Generally, materials increase in volume when subjected to a tensile strain resulting in a ν less than 0.50. For most materials ν lies between 0.2 and 0.5 and approaches 0.50 for rubbers or liquids.

When the material is subjected to a strain sufficiently large to prohibit the use of infinitesimal strain theory, ν is no longer a constant but a function of the strain:

$$\nu = \frac{1}{\alpha - 1}\left[1 - \left(\frac{V}{V_o}\right)^{1/2}\right]\alpha^{-1/2} \qquad (1.2)$$

where ν = Poisson's ratio

α = Principal extension ratio $(1 + \epsilon_1)$

ϵ_1 = Strain

V = Volume

V_o = Original volume

If the material is incompressible, i.e., $V/V_o = 1$, equation (1.2) reduces to:

$$\nu = \frac{1}{\epsilon_1}\left[1 - (1 + \epsilon_1)^{-1/2}\right] \qquad (1.3)$$

It can be seen from equation (1.2) that the lower the value of ν, the greater the volume increase and, hence, the density change due to the strain, ϵ_1. Using these three equations, three propellants have been investigated to date; and a fourth propellant will be studied during the next period.

An apparatus for the determination of the volumetric changes of propellant has been developed and consists of a point light source, an end bonded cylindrical tensile specimen[2], a 10X lens, an Instron tensile tester, and a sheet of graph paper. This is shown schematically in Figure 14. A specimen of known diameter is placed in the path of the point light source. The image is magnified ten times by means of the lens and projected on the graph paper. The highly magnified diameter is measured and the volumetric changes are calculated from the measured lateral and longitudinal strains.

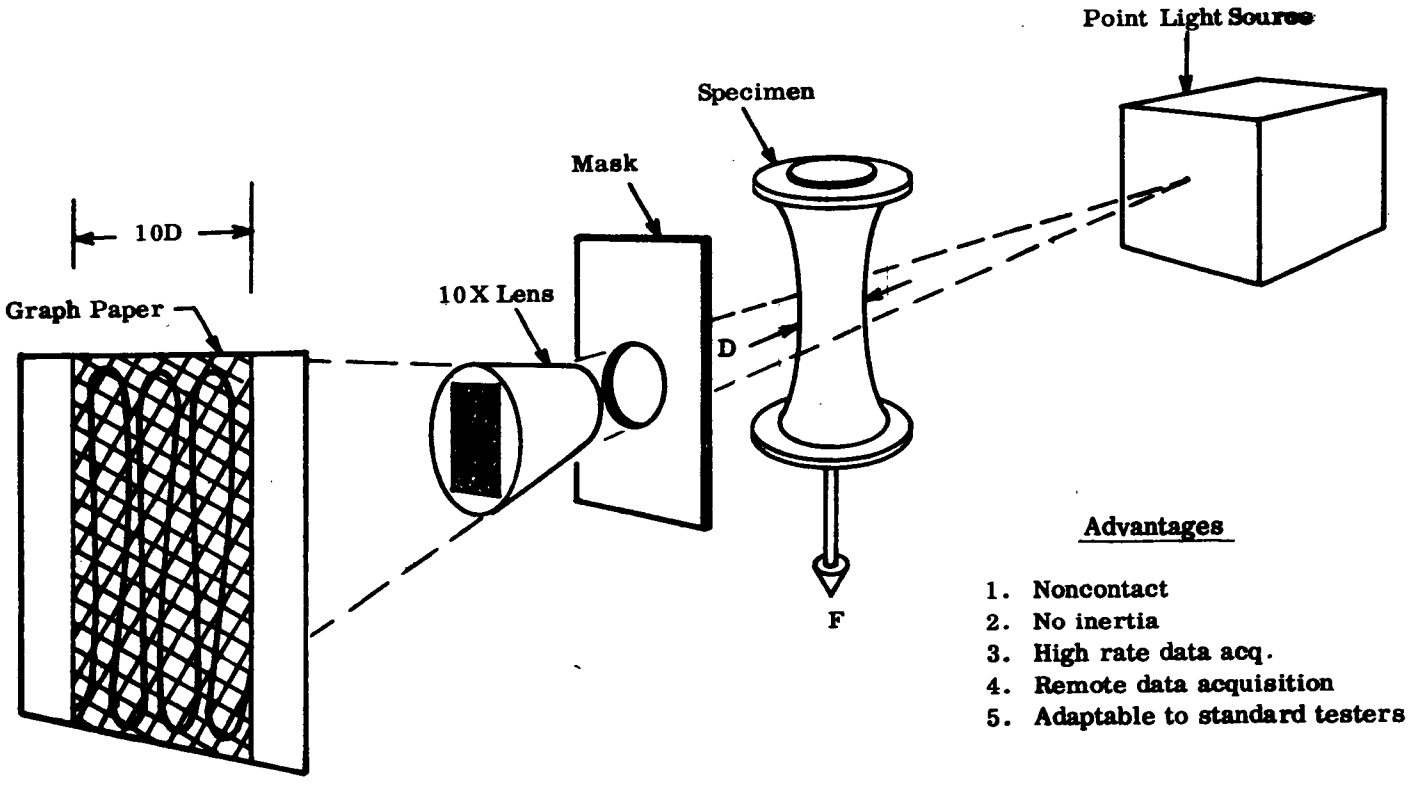

FIGURE 14. APPARATUS FOR MEASURING CROSS SECTIONAL AREA OF A SPECIMEN DURING A TENSILE TEST

Three propellants, in addition to the TP-H-1050 already studied, have been selected for these tests: TP-J-3000 (plastisol), TP-G-3133 (polyurethane), and a modified TP-H-1011(hydrocarbon).The latter was formulated to give a JANAF modulus equal to approximately 1000 psi, so as to obtain a more rigid material for comparative purposes.

Poisson's ratio values as a function of strain are shown in Table XV and Figure 15. From the figure, it can be seen that TP-H-1050 follows very closely the curve for an incompressible material obtained using equation (1.3). The curves for the TP-G-3133, TP-H-1011, and TP-J-3000 propellants, respectively, show increasing deviations from incompressibility. Poisson's ratio for TP-J-3000 at 10 percent strain only has been obtained to date. Additional tests will be made during the final quarter so that this curve can be more fully described. The data on TP-G-3133 and the modified TP-H-1011 represent one test at each strain level. At least five tests at each strain will be made on each propellant before the final curves are established.

B. Strand Burning Rates

The technique employed to study the effects of strain on burning rate was previously reported.[3] Several 1/4 x 1/4 x 6 inch strands are elongated to three different strain levels, 4, 8, and 12 1/2 percent, and burned at nominal pressures of 500, 900, and 1200 psi. The strain level is accomplished by using a constant strain device capable of independently straining two strands. The specimen ends are inserted through Teflon collars and bonded so as to be similar to end-bonded tensile specimens. Once the desired strain level is achieved, the sample is coated on all sides with Armstrong A-1 cement. After curing the coating is relatively stiff and the strain level in the strand is maintained. The burning test is accomplished in a conventional strand burner.

TABLE XV

POISSON'S RATIO VERSUS STRAIN

Test Temperature: 77°F

Percent Strain	TP-G-3133	TP-H-1011	TP-J-3000	TP-H-1050
2	0.479	0.478	-	0.496
4	0.470	0.445	-	0.485
6	0.465	0.425	-	0.463
8	0.460	0.416	-	0.459
10	0.4553	0.409	0.325	0.455
12	0.451	0.405	-	0.462
14	-	-	-	0.464
18	-	-	-	0.456

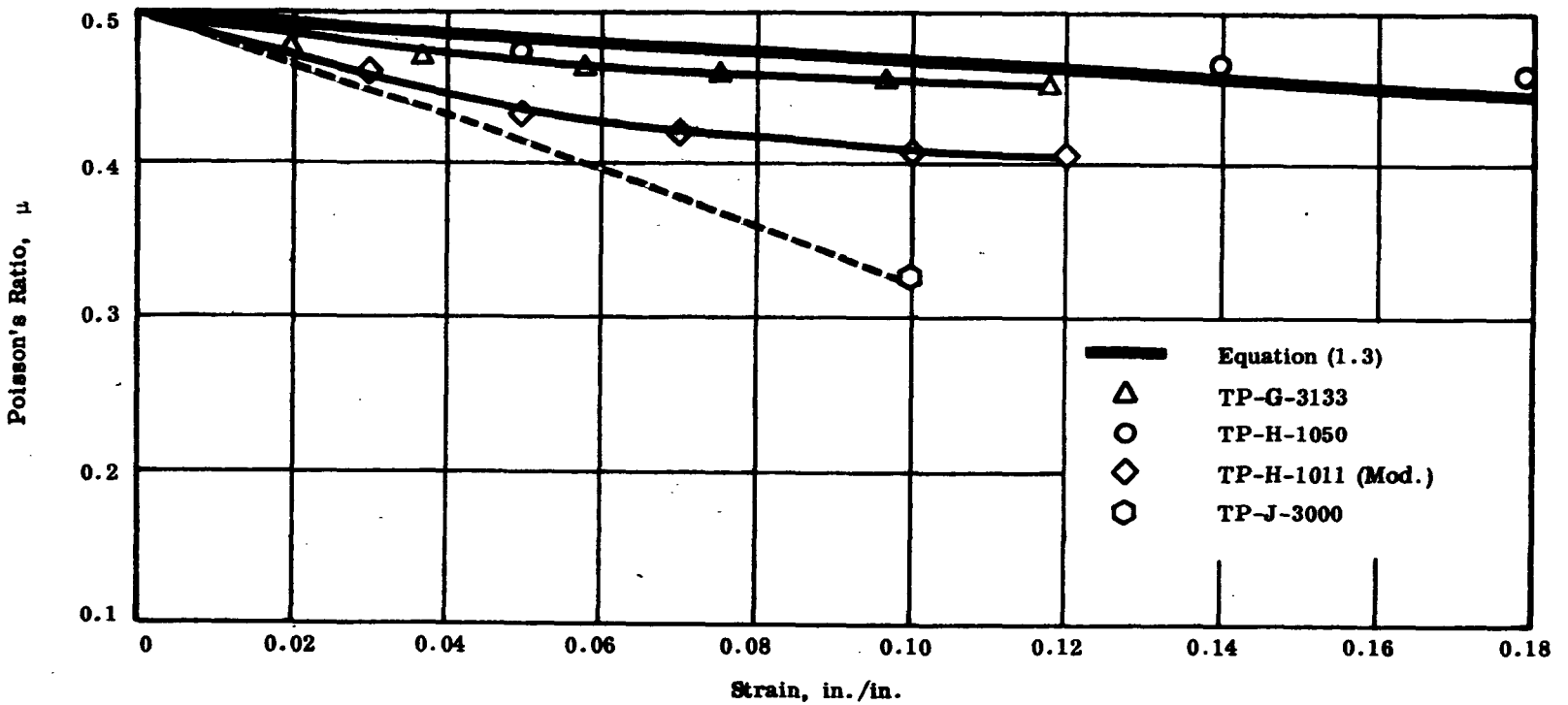

FIGURE 15. POISSON'S RATIO VERSUS STRAIN

Strain Rate: 2.0 in./min
Test Temp: 77°F

The results of the burning rate tests are given in Tables XVI and XVII and illustrated in Figure 16. The data on the plastisol propellant, TP-J-3000, were obtained from a Thiokol-Redstone Division report[4] and represent the effect of approximately 10 percent strain on the burning rate. The latter data are used at this time for comparative purposes only since it is planned to retest this material at this facility during the next quarter in accordance with the above-mentioned test procedure. The effect of the strain on the burning rate of TP-J-3000 is clearly shown. At 1000 psi pressure there is an increase of 33 percent or about 3.3 percent for each percent strain.

TP-G-3133, whose Poisson's ratio deviates only slightly from incompressible behavior, also exhibits a strain sensitivity on its burning rate but to a much lower degree than the plastisol. The increase in burning rate for this formulation at a pressure of 1000 psi at 10 percent strain is about 4.3 percent or 0.43 percent increase for each percent strain.

Burning rate tests on the modified TP-H-1011 have not yet been run. However, since its Poisson's ratio at 10 percent strain falls between that of TP-G-3133 and the TP-J-3000, its strain sensitivity on the burning rate should fall between 0.43 and 3.3 percent. These results will be obtained during the forthcoming quarter.

C. Effect of Strain on Mass Burning Rate

The effect of strain on mass burning rate is also being considered. When a strain is imposed on a strand it will produce an increase in the time necessary to completely burn the propellant (i.e., a 10-percent strain would cause a 10-percent longer

TABLE XVI

BURNING RATE OF TP-G-3133 - 0% STRAIN

Test Number	Average Pressure, psi	Burning Rates in in./sec, 0 - 2 1/2 in.	2 1/2 - 5 in.	Average
1	575	0.158	0.163	0.160
2	550	0.153	0.164	0.157
3	538	0.159	0.155	0.157
4	538	0.157	0.157	0.157
5	500	0.160	0.157	0.158
			A_v =	0.1578
6	1075	0.158	0.161	0.159
7	1075	0.159	0.163	0.161
8	1088	0.166	0.161	0.163
9	1075	0.164	0.159	0.162
10	1063	0.162	-	0.162
			A_v =	0.1616

TABLE XVII

BURNING RATE OF TP-G-3133 - 10% STRAIN

Test Number	Average Pressure, psi	Burning Rates in in./sec, 0 - 2 1/2 in.	2 1/2 - 5 in.	Average
1	538	0.159	0.161	0.160
2	530	0.158	0.160	0.159
3	530	0.156	0.162	0.161
			A_v =	0.160
5	1068	0.163	0.169	0.166
6	1050	0.170	0.170	0.170
7	1075	0.170	0.165	0.168
8	1063	0.164	0.170	0.167
			A_v =	0.168

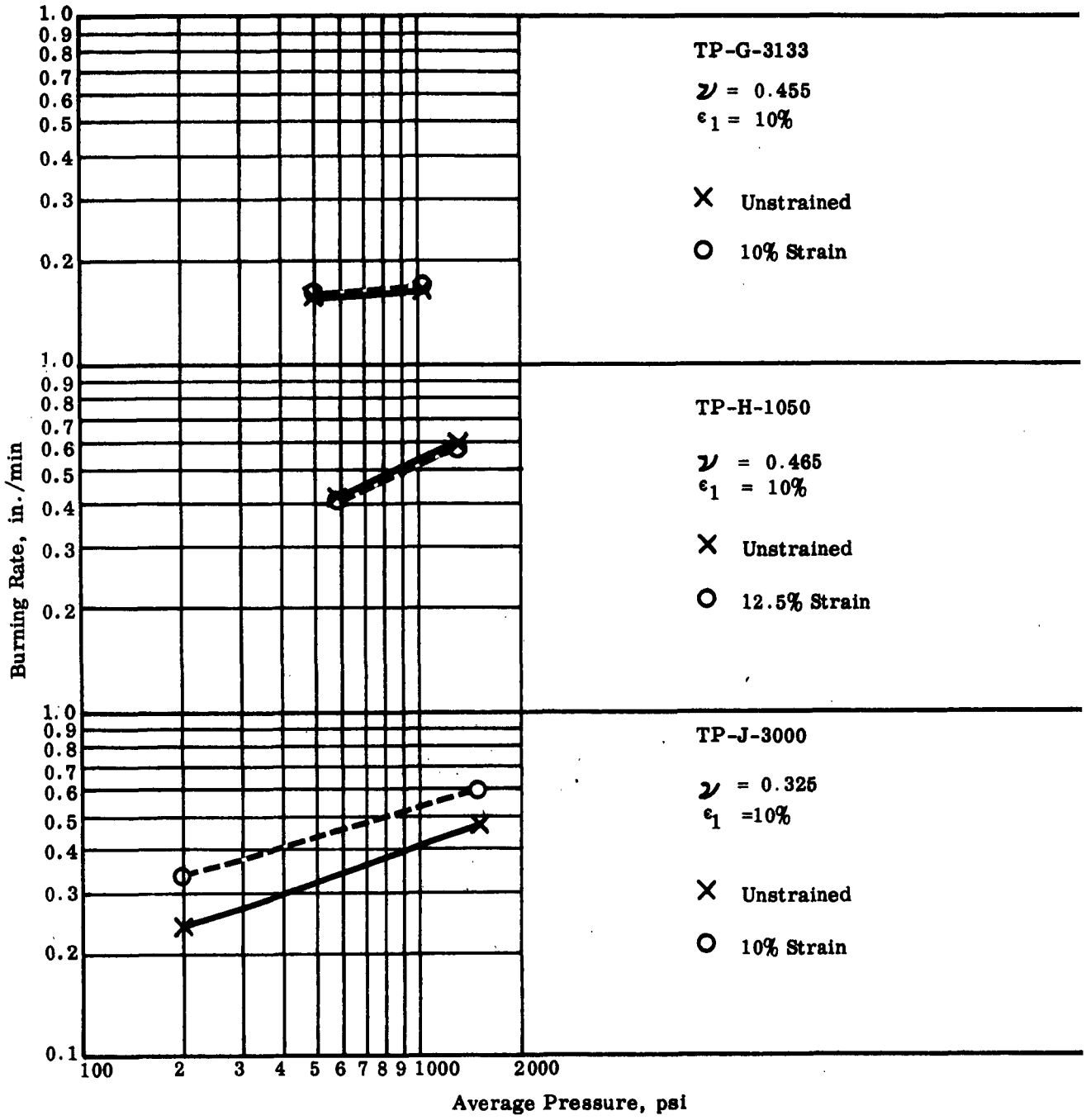

FIGURE 16. BURNING RATE VERSUS PRESSURE

burning time for an incompressible material exhibiting no linear burning rate dependency on strain). The mass burning rate is thus reduced by the time increase required to consume the sample. Therefore, mass burning rate is a direct function of the reciprocal of the strain for the incompressible case.

The linear burning rate generated from TP-H-1050 has indicated that this linear rate is independent of strain up to 12 1/2 percent. Therefore, a 12 1/2-percent strain on a strand would cause a 12 1/2-percent longer burn time.

When the linear burning rate changes with strain, as in the case of TP-G-3133, a more complex relationship exists. Considering the Poisson's ratio values of the modified TP-H-1011 and TP-J-3000, it is expected that a similar relationship will exist due to a greater sensitivty of the burning rate to strain. These propellants will be analyzed as soon as all the burning rate data are available.

IV. PROPELLANT SLUMP ANALYSIS

Principal effort in this area during the past quarter has been directed toward the development of an elastic analysis for a finite length, cylindrical-type grain possessing a spherical head end and undergoing an acceleration in the longitudinal direction (see Figure 17). An approximate numerical technique originally developed by Southwell[5] and more recently extended to rocket grains by Parr,[6,7] Messner and Shearly[11] was found to be especially applicable to the solution of this problem.

The pertinent equations, boundary conditions, and finite difference approximations are described below.

The initial step in any stress-strain-displacement analysis of a solid propellant rocket grain is to obtain a solution of the elastic field equations subject to given boundary conditions and a prescribed external loading. In particular, if the grain is symmetrical with respect to its longitudinal axis and is under a constant acceleration load in the axial direction, the governing system is considerably simplified.

There are a number of methods that may be used to solve this system[8,9]. However, all have inherent difficulties. This may be attributed to the fact that, in essence, the mixed boundary conditions typical of this class of problems must be satisfied.

In the following analysis, it will be assumed that the plane lamina of Figure 17 is an axial cross section of a cylindrical grain capped by a spherical head end and having a straight-through port. It will further be assumed that the propellant charge is linear elastic, isotropic, and homogeneous, and is bonded to a rigid case on its outer periphery (C') and head end (D'). The stresses, strains, and displacements to be

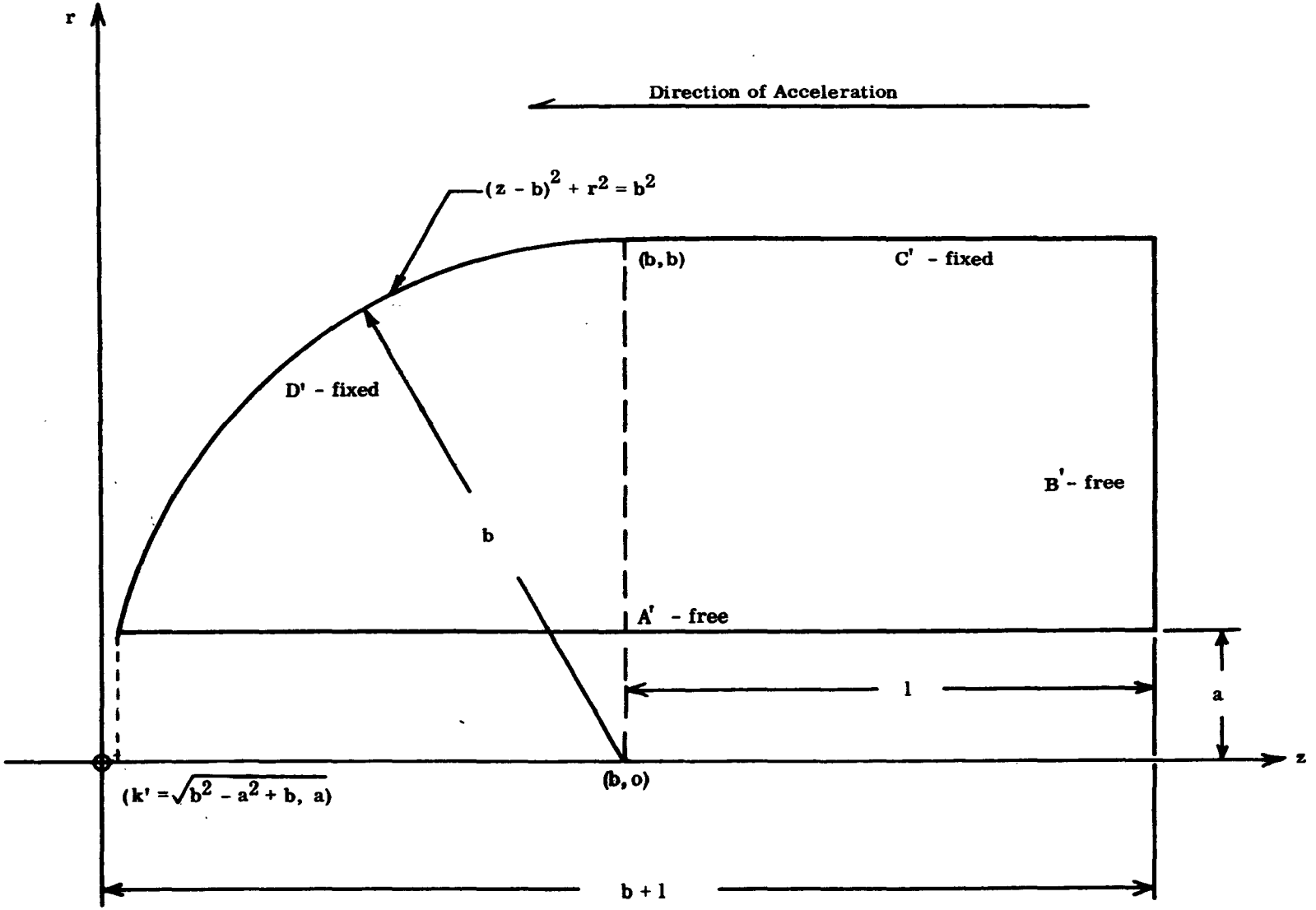

FIGURE 17. CYLINDRICAL GRAIN WITH SPHERICAL HEAD END

determined are those induced by a constant acceleration load applied in the longitudinal direction.

A. Stress Functions

It has been shown[5, 10] that elastic bodies having forms that are solids of revolution and loaded so that axial symmetry is maintained in the resulting deformation are amenable to numerical solution using stress functions and relaxation techniques. In particular, for the conditions described above, if two functions, $\underset{\sim}{\Phi}$ and $\underset{\sim}{\Psi}$, of the spacial coordinates r and z (but not $\tilde{0}$)* are defined in such a way that they satisfy the differential system

$$\frac{\partial^2 \underset{\sim}{\Phi}}{\partial r^2} - \frac{1}{r}\frac{\partial \underset{\sim}{\Phi}}{\partial r} + \frac{\partial^2 \underset{\sim}{\Phi}}{\partial z^2} = 0$$

$$\frac{\partial^2 \underset{\sim}{\Psi}}{\partial r^2} - \frac{1}{r}\frac{\partial \underset{\sim}{\Psi}}{\partial r} + \frac{\partial^2 \underset{\sim}{\Psi}}{\partial z^2} = \frac{\partial^2 \underset{\sim}{\Phi}}{\partial z^2} \qquad (2.1)$$

then the equilibrium and compatibility conditions are satisfied if the stresses are defined by[5]

$$\sigma_r = \frac{1}{r}\left[\frac{\partial \underset{\sim}{\Phi}}{\partial r} + \frac{\partial \underset{\sim}{\Psi}}{\partial r}\right] - \frac{1}{r^2}\left[\underset{\sim}{\Psi} + (1-\nu)\underset{\sim}{\Phi}\right] \qquad (2.2)$$

$$\sigma_{\tilde{\theta}} = \frac{\nu}{r}\frac{\partial \underset{\sim}{\Phi}}{\partial r} + \frac{1}{r^2}\left[\underset{\sim}{\Psi} + (1-\nu)\underset{\sim}{\Phi}\right] \qquad (2.3)$$

$$\sigma_z = -\frac{1}{r}\frac{\partial \underset{\sim}{\Psi}}{\partial r} + z\, I_z \qquad (2.4)$$

and

---

* See Nomenclature, p. 65

$$\tau_{rz} = \frac{1}{r}\frac{\partial \Psi}{\partial z} \tag{2.5}$$

I_z is the effective body force due to acceleration and is equal to the load in "g"s multiplied by the mass density of the propellant.

The associated strains and displacements, expressed as functions of Φ, Ψ and their partial derivations, may be obtained from the axisymmetric stress-strain and strain-displacement relations of elasticity. For reasons of brevity these are not included here.

B. Cylindrical Grain with Spherical Head End

Using standard notation[6,7], we define (see Figure 17)

$$\rho = \frac{r}{b} \qquad \sigma_\rho = \frac{\sigma_r}{E} \qquad \epsilon_\rho = \epsilon_r$$

$$\eta = \frac{z}{b} \qquad \sigma_\theta = \frac{\sigma\tilde{\theta}}{E} \qquad \epsilon_\theta = \epsilon\hat{\theta}$$

$$Z = \frac{bI_z}{E} \qquad \sigma_\eta = \frac{\sigma_z}{E} \qquad \epsilon_\eta = \epsilon_z$$

$$\Phi = b^2 E \phi \qquad \tau_{\rho\eta} = \frac{\tau_{rz}}{E} \qquad \gamma_{\rho\eta} = \gamma_{rz}$$

$$\Psi = b^2 E \psi \qquad u\rho = \frac{u}{b} \qquad u_\eta = \frac{w}{b}$$

in order that the governing equations (2.1), stresses (2.2)-(2.5), strains and displacements may be expressed in a more compact nondimensional form. These may now be written as

$$\frac{\partial^2 \phi}{\partial \rho^2} - \frac{1}{\rho}\frac{\partial \phi}{\partial \rho} + \frac{\partial^2 \phi}{\partial \eta^2} = 0$$

$$\frac{\partial^2 \psi}{\partial \rho^2} - \frac{1}{\rho}\frac{\partial \psi}{\partial \rho} + \frac{\partial \psi}{\partial \eta^2} = \frac{\partial^2 \phi}{\partial \eta^2} \tag{2.6}$$

and

$$u_\rho = \frac{(1+\nu)}{\rho}\left[\psi + (1-\nu)\,\phi\right] - \nu\,\rho\eta Z \tag{2.7}$$

$$u_\eta = -\frac{(1+\nu)}{\rho}\left[\int_{\eta=k'}^{\eta} \frac{\partial \psi}{\partial \rho}\, d\eta + \nu \int_{\eta=k'}^{\eta} \frac{\partial \phi}{\partial \rho}\, d\eta\right] - \frac{k'^2 Z}{2} + \frac{\eta^2 Z}{2} + f(\rho) \tag{2.8}$$

$$\epsilon_\rho = \frac{(1+\nu)}{\rho}\left\{\frac{\partial \psi}{\partial \rho} + (1-\nu)\frac{\partial \phi}{\partial \rho} - \frac{1}{\rho}\left[\psi + (1-\nu)\,\phi\right]\right\} - \nu\eta Z \tag{2.9}$$

$$\epsilon_\theta = \frac{(1+\nu)}{\rho^2}\left[\psi + (1-\nu)\,\phi\right] - \nu\eta Z \tag{2.10}$$

$$\epsilon_\eta = -\frac{(1+\nu)}{\rho}\left[\frac{\partial \psi}{\partial \rho} + \nu\,\frac{\partial \phi}{\partial \rho}\right] + \eta Z \tag{2.11}$$

$$\sigma_\rho = \frac{1}{\rho}\left[\frac{\partial \phi}{\partial \rho} + \frac{\partial \psi}{\partial \rho}\right] - \frac{1}{\rho^2}\left[\psi + (1-\nu)\,\phi\right] \tag{2.12}$$

$$\sigma_\theta = \frac{\nu}{\rho}\,\frac{\partial \phi}{\partial \rho} + \frac{1}{\rho^2}\left[\psi + (1-\nu)\,\phi\right] \tag{2.13}$$

$$\sigma_\eta = -\frac{1}{\rho}\,\frac{\partial \psi}{\partial \rho} + \eta Z \tag{2.14}$$

$$\tau_{\rho\eta} = \frac{1}{\rho}\,\frac{\partial \psi}{\partial \eta} \tag{2.15}$$

$$\gamma_{\rho\eta} = \frac{2(1+\nu)}{\rho}\,\frac{\partial \psi}{\partial \eta} \tag{2.16}$$

$f(\rho)$ in (1.8) was found to be equal to

$$f(\rho) = \int_{k'}^{\rho}\left[\frac{1+\nu}{\rho}\,\frac{\partial \psi}{\partial \eta} - \frac{1-\nu^2}{\rho}\,\frac{\partial \phi}{\partial \eta}\right]d\rho + \left\{\frac{1+\nu}{\rho}\left[\int_{k'}^{\eta}\frac{\partial \psi}{\partial \rho}\,d\eta + \nu\int_{k'}^{\eta}\frac{\partial \phi}{\partial \rho}\,d\eta\right]\right\}\Bigg|_{k'}^{\rho} + \frac{\nu Z}{2}\left[\rho^2 - k'^2\right] \tag{2.17}$$

The simultaneous solution of (2.6) subject to the boundary conditions described above and illustrated in Figure 18 constitutes a description of the stress-strain-displacement state of the propellant charge. The boundary conditions are delineated below.

Side A ($\rho = \alpha$)

On this boundary the normal radial stress and the shearing stress are identically zero and hence

$$\sigma_\rho = 0 \tag{2.18}$$

$$\tau_{\rho\eta} = 0 \tag{2.19}$$

Side B ($\eta = H$)

On this free boundary the normal axial stress and the shearing stress are identically zero and hence

$$\sigma_\eta = 0 \tag{2.20}$$

$$\tau_{\rho\eta} = 0 \tag{2.21}$$

Side C ($\rho = 1$)

On this fixed boundary the radial and axial displacements are identically zero and hence

$$u_\rho = 0 \tag{2.22}$$

and

$$u_\eta = 0 \tag{2.23}$$

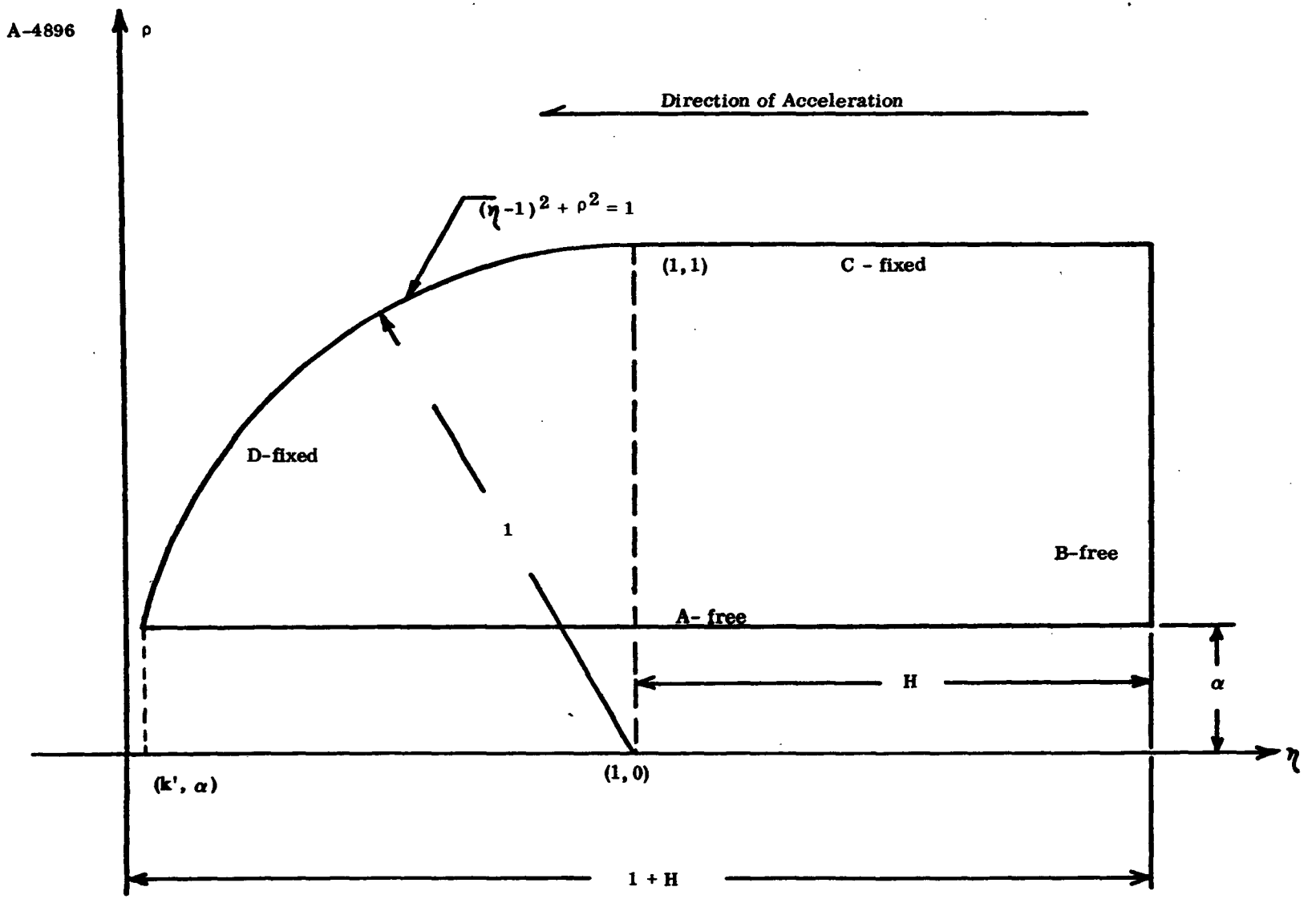

$$\alpha = \frac{a}{b}\ ;\ H = \frac{l}{b}\ ;\ k' = \sqrt{(1-\rho^2)} + 1$$

FIGURE 18. DIMENSIONLESS COORDINATE SYSTEM

Side D [$\rho = f(\eta)$]

On this curved spherical boundary the radial and axial displacements are again zero and hence

$$u_\rho = 0 \tag{2.24}$$

and

$$u_\eta = 0 \tag{2.25}$$

Corner Points

At these points the boundary conditions for each pair of adjoining boundaries must be satisfied.

C. Finite Difference Approximations

1. Governing System

Upon considering the nodal molecule of Figure 19, it is readily seen that the finite difference representation of (2.6) in relation to the central node is

$$\frac{h}{2\rho_o}(\phi_4 - \phi_2) + \phi_1 + \phi_2 + \phi_3 + \phi_4 - 4\phi_o = 0$$

$$\frac{h}{2\rho_o}(\psi_4 - \psi_2) + \psi_1 + \psi_2 + \psi_3 + \psi_4 - 4\psi_o - \phi_1 - \phi_3 + 2\phi_o = 0 \tag{3.1}$$

The question arises as to what alterations must be made in (3.1) when one or more of the points of a nodal molecule lies outside the boundary of the grain. Such points, aptly termed fictitious, are present for both boundary nodes and interior nodes when such nodes are separated from adjacent nodes by a boundary.

It is clear that if the curved portion of the boundary lies to the left of the

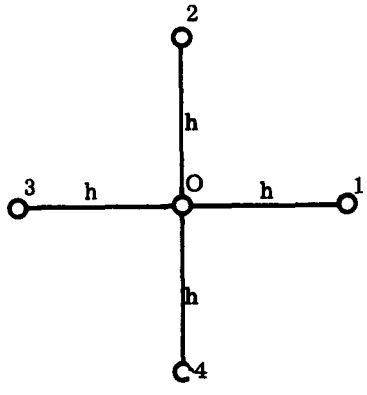

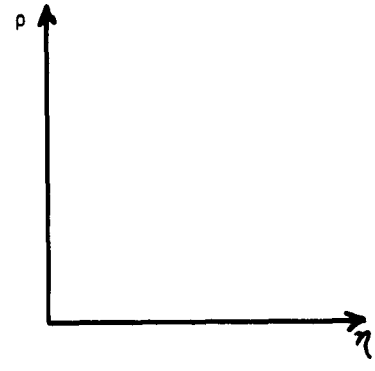

$$\left(\frac{\partial X}{\partial \rho}\right)_o = \frac{X_2 - X_4}{2h}$$

$$\left(\frac{\partial X}{\partial \eta}\right)_o = \frac{X_1 - X_3}{2h}$$

$$\left(\frac{\partial^2 X}{\partial \rho^2}\right)_o = \frac{X_2 + X_4 - 2X_o}{h^2}$$

$$\left(\frac{\partial^2 X}{\partial \eta^2}\right)_o = \frac{X_1 + X_3 - 2X_o}{h^2}$$

FIGURE 19. FINITE DIFFERENCE MOLECULE

mid-section as it does in Figure 18, then in reference to nodes centered in the interior there are three possibilities; namely,

(1) Nodes 2 and 3 are fictitious

(2) Node 2 is fictitious

(3) Node 3 is fictitious

Consider the first case, which is illustrated in Figure 20a. Without loss of generality it may be assumed that ϕ and ψ can be expanded in a two-dimensional Taylor series of the form

$$X = X_o + \eta \left(\frac{\partial X}{\partial \eta}\right)_o + \rho \left(\frac{\partial X}{\partial \rho}\right)_o + \frac{\eta^2}{2} \left(\frac{\partial X}{\partial \eta^2}\right)_o + \qquad (3.2)$$

$$\rho\eta \left(\frac{\partial^2 X}{\partial \rho \partial \eta}\right)_o + \frac{\rho^2}{2} \left(\frac{\partial^2 X}{\partial \rho^2}\right)_o + \text{---}$$

The fictitious nodes 2 and 3 must be replaced by the boundary nodes A and B. If it is assumed that the origin of the coordinate system has for the moment been translated to node O, then the points 1, 4, A, B have coordinates (h, 0), (0, -h), $(-\delta_A h, 0)$ and $(0, \delta_B h)$. When substituted into (3.2), these provide four linear equations in terms of the first and second derivatives of ϕ and ψ at node O as follows:

$$X_1 = X_o + h\left(\frac{\partial X}{\partial \eta}\right)_o + \frac{h^2}{2} \left(\frac{\partial^2 X}{\partial \eta^2}\right)_o \qquad (3.2a)$$

$$X_4 = X_o - h \left(\frac{\partial X}{\partial \rho}\right)_o + \frac{h^2}{2} \left(\frac{\partial^2 X}{2\rho^2}\right)_o \qquad (3.2b)$$

A-4893

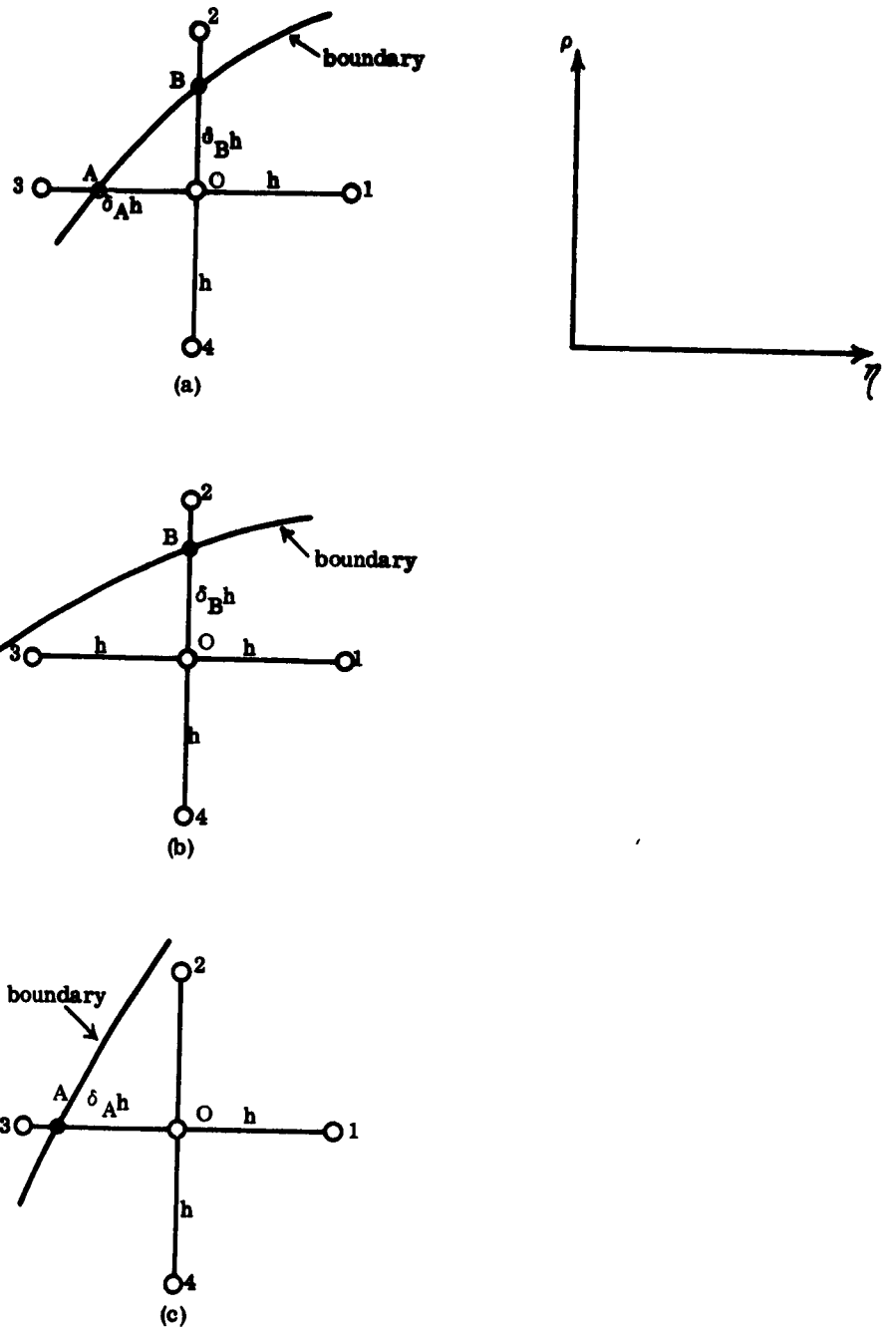

FIGURE 20. IRREGULAR MOLECULES

$$X_A = X_o - \delta_A h \left(\frac{\partial X}{\partial \eta}\right)_o + \frac{(\delta_A h)^2}{2} \left(\frac{\partial^2 X}{\partial \eta^2}\right)_o \qquad (3.2c)$$

$$X_B = X_o + (\delta_B h)\left(\frac{\partial X}{\partial \rho}\right)_o + \frac{(\delta_B h)^2}{2}\left(\frac{\partial^2 X}{\partial \rho^2}\right)_o \qquad (3.2d)$$

When these systems are solved simultaneously for the first and second derivatives of ϕ, σ and ψ at node O, the governing equations (3.1) are found to be of the form

$$K_1\phi_1 + K_2\phi_B + K_3\phi_A + K_4\phi_4 + K_5\phi_o = 0 \qquad (3.3)$$

$$K_1\psi_1 + K_2\psi_B + K_3\psi_A + K_4\psi_4 - K_5\psi_o - \frac{K_1}{\delta_A}\phi_A - K_1\phi_1 - \left(\frac{K_1}{\delta_A} - K_1\right)\phi_o = 0$$

where K_i (i = 1,5) are constants to be computed for each such node. They are:

$$K_1 = \frac{2}{1+\delta_A}$$

$$K_2 = -\frac{2\rho_o + h}{\rho_o \delta_B (1+\delta_B)}$$

$$K_3 = \frac{K_1}{\delta_A}$$

$$K_4 = \frac{2\rho_o + \delta_B h}{\rho_o (1+\delta_B)}$$

$$K_5 = 2\left[\frac{1-\delta_A}{\delta_A(1+\delta_A)} + \frac{1-\delta_B}{\delta_B(1+\delta_B)} + \frac{h}{2\rho_o}\left(\frac{1-\delta_B}{\delta_B}\right)\right]$$

Similar expressions for case 2 (Figure 20b) and case 3 (Figure 20c) may be derived in an analogous manner.

2. Stresses, Strains and Displacements

The stresses, strains, and radial displacement in finite difference form (relative to an arbitrary node O were found to be:

$$(\sigma_\rho)_o = \frac{1}{2h\rho_o}\left[\phi_2 - \phi_4 + \psi_2 - \psi_4\right] - \frac{1}{\rho_o^2}\left[\psi_o + (1-\nu)\,\phi_o\right] \quad (3.4)$$

$$(\sigma_\theta)_o = \frac{\nu}{2h\rho_o}\left[\phi_o - \phi_4\right] + \frac{1}{\rho_o^2}\left[\psi_o + (1-\nu)\,\phi_o\right] \quad (3.5)$$

$$(\sigma_\eta)_o = -\frac{1}{2h\rho_o}\left[\psi_2 - \psi_4\right] + \eta_o Z \quad (3.6)$$

$$(\tau_{\rho\eta})_o = \frac{1}{2h\rho_o}\left[\psi_1 - \psi_3\right] \quad (3.7)$$

$$(\varepsilon_\theta)_o = \frac{(1+\nu)}{\rho_o^2}\left[\psi_o + (1-\nu)\,\phi_o\right] - \nu\eta_o Z \quad (3.8)$$

$$(\varepsilon_\rho)_o = \frac{(1+\nu)}{2h\rho_o^2}\left\{\rho_o(\psi_2 - \psi_4) + \rho_o(1-\nu)(\phi_2 - \phi_4) - 2h\left[\psi_o + (1-\nu)\,\phi_o\right]\right\} - \nu\eta_o Z \quad (3.9)$$

$$(\varepsilon_\eta)_o = -\frac{(1+\nu)}{2h\rho_o}\left[\psi_2 - \psi_4 + \nu(\phi_2 - \phi_4)\right] + \eta_o Z \quad (3.10)$$

$$(u_\rho)_o = \frac{(1+\nu)}{\rho_o}\left[\psi_o + (1-\nu)\phi_o\right] - \nu\rho_o\eta_o Z \quad (3.11)$$

3. Boundary Conditions

The boundary conditions in finite difference form for sides A and B are the same as those given by Parr[6] for the free boundaries of the cylinders he studied. They are:

Side A ($\rho = \alpha$)

$$\psi_o = 0 \tag{3.12}$$

$$\phi_2 + \psi_2 - \left\{1 + (1 - \nu)\frac{h}{\alpha}\left[1 + \frac{h}{2\alpha}\right]\right\} \phi_o = 0 \tag{3.13}$$

Side B ($\eta = H$)

$$\psi_o = \frac{(\rho_o^2 - \alpha^2)}{2} HZ \tag{3.14}$$

$$2\psi_3 + \frac{h}{2\rho_b}\left[\phi_4 - \phi_2\right] + \phi_2 + \phi_4 - 2\phi_o - 2\psi_o = 0 \tag{3.15}$$

Side C ($\rho = 1$)

On this fixed boundary it follows immediately using (2.22) and (3.11) that one condition which the stress functions must satisfy is

$$\phi_o = -\frac{1}{1-\nu}\left[\psi_o - \frac{\nu \eta_o Z}{1+\nu}\right] \tag{3.16}$$

u_η is also identically zero on this boundary and since u_η is invariant with respect to η here, this implies that ϵ_η is also zero. Thus, after using (3.1) to eliminate the fictitious values ϕ_2, ψ_2 in (3.10), the second condition which the stress functions must satisfy is seen to be:

$$\begin{aligned} &\psi_1 + \psi_3 + 2\psi_4 - 4\psi_o - (1-\nu)\phi_1 - (1-\nu)\phi_3 \\ &+ 2\nu\phi_4 + 2(1-2\nu)\phi_o - h\frac{(h-2)}{1+\nu}\eta_o Z = o \end{aligned} \tag{3.17}$$

Side D $\left[\rho = f(\eta)\right]$

On this boundary u_ρ is again zero and the first condition which the stress functions must satisfy is the same as (3.16). Namely,

$$\phi_o = -\frac{1}{1-\nu}\left[\psi_o - \frac{\nu \eta_o Z}{1+\nu}\right] \tag{3.18}$$

The second boundary condition (2.25) when applied to (2.8) does not present a form that is attractive from a numerical standpoint. However, since u_η is invariant with respect to arc length on this boundary

$$\frac{\partial u_\eta}{\partial s} = 0 \tag{3.19}$$

But

$$\frac{\partial u_\eta}{\partial s} = \frac{\partial u_\eta}{\partial \eta}\frac{d\eta}{ds} + \frac{\partial u_\eta}{\partial \rho}\frac{d\rho}{ds} \tag{3.20}$$

Hence, using (3.19) and (3.20)

$$\frac{\partial u_\eta}{\partial \eta} = -\frac{\partial u_\eta}{\partial \rho}\frac{d\rho}{d\eta} \tag{3.21}$$

Now

$$\frac{\partial u_\eta}{\partial \eta} = \epsilon_\eta = -\frac{(1+\nu)}{\rho}\left[\frac{\partial \psi}{\partial \rho} + \nu \frac{\partial \phi}{\partial \rho}\right] + \eta Z \tag{3.22}$$

$$\frac{\partial u_\eta}{\partial \rho} = \gamma_{\rho\eta} - \frac{\partial u_\rho}{\partial \eta} \tag{3.23}$$

$$\gamma_{\rho\eta} = 2\frac{(1+\nu)}{\rho}\frac{\partial \psi}{\partial \eta} \tag{3.24}$$

and

$$\frac{\partial u_\rho}{\partial \eta} = \frac{(1+\nu)}{\rho}\left[\frac{\partial \psi}{\partial \eta} + (1-\nu)\frac{\partial \phi}{\partial \eta}\right] - \nu \rho Z \tag{3.25}$$

Noticing that on this boundary

$$\frac{d\psi}{d\eta} = \frac{1-\eta}{\rho} \tag{3.26}$$

and employing (3.22) - (3.26) a more tractable boundary condition is obtained. Namely,

$$\frac{\partial \Psi}{\partial \rho} + \nu \frac{\partial \phi}{\partial \rho} - \left\{ \frac{\partial \Psi}{\partial \eta} - (1-\nu) \frac{\partial \phi}{\partial \eta} \right\} \cdot \frac{(1-\eta)}{\rho} - \frac{\rho Z}{(1+\nu)} \left[(1-\nu)\eta + \nu \right] \tag{3.27}$$

Using backward differences, it is found that in finite difference form (4.26) may be expressed as

$$\Psi_0 - \Psi_4 + \nu (\phi_0 - \phi_4) - \left[\Psi_0 - \Psi_1 - (1-\nu) \left\{ \phi_0 - \phi_1 \right\} \right] \cdot \frac{(1-\eta_0)}{\rho_0}$$

$$- \frac{\rho_0 h Z}{(1+\nu)} \left[(1-\nu)\eta_0 + \nu \right] = 0 \tag{3.28}$$

Corner Nodes:

The satisfaction at adjoining boundaries of the boundary conditions defined above consists mainly of algebraic manipulations of said relations. For purposes of brevity and since considerable effort is yet needed in defining the computer logic that must be developed in order to make the above analysis practicable, these conditions are not included at this time.

NOMENCLATURE

$r, \tilde{\theta}, z$	-	Cylindrical coordinates
ρ, θ, η	-	Dimensionless cylindrical coordinates
u	-	Radial displacement (in.)
u_ρ	-	Radial displacement (dimensionless)
W	-	Axial displacement
u_η	-	Axial displacement (dimensionless)
σ_r	-	Radial stress (psi)
σ_ρ	-	Radial stress (dimensionless)
σ_z	-	Axial stress (psi)
σ_η	-	Axial stress (dimensionless)
$\sigma_{\tilde{\theta}}$	-	Tangential stress (psi)
σ_θ	-	Tangential stress (dimensionless)
τ_{rz}	-	Shear stress (psi)
$\tau_{\rho\eta}$	-	Shear stress (dimensionless)
ϵ_r	-	Radial strain (in./in.)
ϵ_ρ	-	Radial strain (dimensionless)
ϵ_z	-	Axial strain (in./in.)
ϵ_η	-	Axial strain (dimensionless)
$\epsilon_{\tilde{\theta}}$	-	Tangential strain (in./in.)
ϵ_θ	-	Tangential strain (dimensionless)
γ_{rz}	-	Shear strain (in./in.)
$\gamma_{\rho\eta}$	-	Shear strain (dimensionless)

NOMENCLATURE (Cont'd)

I_z	-	Body force, mass density x acceleration in "g"
Φ, ϕ	-	Stress functions
Ψ, ψ	-	Stress functions
l	-	Length of cylinder (in.)
b	-	Case radius (in.)
a	-	Port radius (in.)
E	-	Elastic modulus (psi)
ν	-	Poisson's ratio
α	=	$\frac{a}{b}$
H	=	$\frac{b + l}{b}$
s	=	Arc length
h	=	Nodal dimension

V. FUTURE WORK

The remaining two-dimensional heat transfer test cases will be completed during the final quarterly period. This will effectively complete the demonstration of this computer program.

The capability of automatically performing a complete grain design analysis with an irregular temperature profile will be installed into the Advanced Grain Design Computer Program after the program is fully checked out for the half star point case.

The relationship between Poisson's ratio behavior and the effect of strain on burning rate will be defined more conclusively. The remaining laboratory testing required to obtain a significant correlation will be accomplished. The analysis of these data will consider both linear and mass burning rates.

Immediate effort in the propellant slump area will be directed toward the definition, by means of flow charts, etc., of the computer logic necessary to obtain numerical results from the analysis described in Section IV of this report.

Complete compilation and documentation of each study area will be accomplished preparatory to the program summary report publication.

BIBLIOGRAPHY

1. "Quarterly Progress Report No. 2," This Contract, Thiokol Chemical Corporation, Elkton Division, Report E13-63 (March 8, 1963).

2. Saylak, D. "Design, Fabrication, and Evaluation of an End Bonded Cylindrical Tensile Dumbbell for Tensile Testing Composite Rocket Propellants," Bulletin of the First Meeting, ICRPG Working Group on Mechanical Behavior, CPIA Publication No. 2, p. 54 (December 1962).

3. "Quarterly Progress Report No. 9," This Contract, Thiokol Chemical Corporation, Elkton Division, Report E173-62 (December 1, 1962).

4. Guzzo, A. T. "Progress Report on the Development of Plastisol Type Propellants," Contract DA-01-021-ORD-4540, ORO Project TU2-3H, Thiokol Chemical Corporation (Redstone Division) Report No. 18-54 (March 1954).

5. Southwell, R. V. "Some Practically Important Stress-Systems in Solids of Revolution," Proceedings of the Royal Society, Series A, Volume 180, pp. 367-386 (1942).

6. Rohm & Haas Company, "Quarterly Progress Report on Engineering Research," No. P-61-17 (June 1962).

7. Parr, C. H. and Gillis, G. F. "Deformations of Case-Bonded Solid Propellant Grains Under Axial and Transverse Acceleration Loads," presented at the A.R.S. Solid Propellant Rocket Conference, Philadelphia (1963).

8. Timoshenko, S. and Goodier, J. N. "Theory of Elasticity," Second Edition; New York: McGraw-Hill (1951).

9. "Modern Mathematics for the Engineer," edited by E. F. Beckenbach, University of California Engineering Extension Series, Volume I & II, McGraw-Hill (1956), (1961).

10. Southwell, R. V. "Relaxation Methods in Theoretical Physics," Oxford (1956).

11. Messner, A. M. and Shearly, R.N. "Stress Analysis of Axisymmetrical Propellant Grains with Arbitrary End Geometries (U)," Transactions of the Seventh Symposium on Ballistic Missile and Space Technology, Volume III (1962), SECRET.